MAGI'S LAB SRL

UNIVERSITÀ
DI SIENA
1240

DEPARTMENT OF BIOTECHNOLOGY,
CHEMISTRY AND PHARMACY

DOCTORAL THESIS IN
BIOCHEMISTRY AND MOLECULAR BIOLOGY
XXXVIII Cycle

Coordinator: Prof. Lorenza Trabalzini

OMICS-Based Profiling in Inherited Retinal Dystrophies: Dissecting Oligogenic Inheritance through Mutational Burden Models and Developing a Plasma Proteome-Based Framework

SCIENTIFIC-DISCIPLINARY SECTOR: BIOS/7

ACADEMIC SUPERVISOR: Prof. Andrea Bernini

INDUSTRIAL SUPERVISOR: Dr. Matteo Bertelli

PhD STUDENT

Medori Maria Chiara

21/03/2026 10:26:21
MARIA CHIARA MEDORI

Academic Year 2024/2025

INDEX

ABSTRACT

Inherited Retinal Dystrophies (IRDs) are a clinically and genetically heterogeneous group of disorders characterized by the progressive degeneration of photoreceptors and retinal pigment epithelium, leading to irreversible vision loss. More than 250 genes have been implicated in IRDs, with inheritance patterns including autosomal dominant, autosomal recessive, and X-linked modes. However, despite the widespread application of next-generation sequencing (NGS), approximately 40% of IRD patients remain genetically unsolved. In many of these cases, only single heterozygous variants in recessive genes are identified, which is insufficient to explain the phenotype under classic Mendelian interpretation. This observation suggests the existence of complex, non-Mendelian inheritance mechanisms such as digenic, triallelic, or oligogenic interactions. The concept of *mutational burden*, which quantifies the cumulative effect of multiple rare variants in functionally related genes, has emerged as a powerful interpretative model for these unresolved cases. In parallel, the clinical progression of IRDs does not follow a linear trajectory. Instead, patients often alternate between stable (latent) phases and rapid-degenerative (active) phases, in the absence of clear genetic or clinical predictors. Plasma proteomics offers a promising avenue to detect early molecular signatures of disease activity, including markers of inflammation, oxidative stress, and cell death. Identifying these transitions is critical for developing therapeutic strategies aimed at halting or delaying vision loss.

This work introduces a model designed to address two major challenges in IRD research and clinical practice: the genetic complexity of unresolved IRD cases and the non-linear dynamics of disease progression. First, we developed a mutational burden model to quantify the aggregate impact of rare heterozygous variants across selected biological pathways, with the aim of identifying patients whose phenotype may be explained by oligogenic inheritance. Second, we developed a machine-learning classifier using plasma proteomic data to distinguish between the active and latent phases of retinal degeneration. These

complementary approaches aim to improve diagnostic yield, enable better patient stratification, and support personalized clinical management.

We analyzed clinical and genetic data from 527 individuals (453 IRD patients and 74 controls). Variants were annotated and classified according to ACMG guidelines, and a pathogenicity score was assigned: pathogenic (P) = 0.5, likely pathogenic (LP) = 0.3, and variants of uncertain significance (VUS HOT) = 0.2. To account for age-dependent expressivity, scores were normalized by age. Using curated databases (KEGG, Reactome, STRING), we mapped the retinal-related molecular pathways. Mutational burden scores were computed as the sum of pathogenicity weights across genes in each pathway. Differences between patients and controls were assessed using the Mann–Whitney U test. Kernel Density Estimation (KDE) was applied to the burden distribution to define the 90th percentile threshold for high-burden classification. Additionally, we identified gene pairs present in patients but absent in controls within significantly burdened pathways, highlighting possible oligogenic interactions.

We also generated a synthetic dataset of 500 plasma proteomic profiles, each containing 315 proteins relevant to IRD pathophysiology. Expression levels were scaled using MinMax normalization. Proteins were grouped into ten biological pathways: inflammation, oxidative stress, immunity, apoptosis, aging, visual perception, ciliopathies, lipid metabolism, cellular transport, and signal transduction. For each sample, a pathway activation score was computed. Samples were classified as “active phase” if at least two pathways exceeded an activation threshold of 0.70; otherwise, they were labeled as “latent phase”. We trained four machine learning models (Logistic Regression, Support Vector Machine, Random Forest, and XGBoost) on 80% of the dataset and evaluated them on the remaining 20% using accuracy, precision, recall, and F1-score. Feature importance was assessed to identify the most informative proteins.

The mutational burden model identified two significantly enriched pathways in the patient group: *Retinoid Cycle Disease Events* ($p = 0.00002$) and *The Canonical Retinoid Cycle in Rods* ($p = 0.012$), with a high correlation ($r = 0.92$). KDE analysis established a 90th percentile burden threshold, above which patients were classified as high-burden. Among these, we identified two gene combinations—*ABCA4–RDH12* and *ABCA4–RBP3*—that are present exclusively in patients. The model enables prioritizing variants for functional validation and reclassifying previously unsolved cases.

About proteomics, the machine learning classifier reached the best performance with Logistic Regression (accuracy: 72%; precision: 0.72; F1-score: 0.71). The most discriminative biomarkers included TIMP3 and VEGFA (inflammation and fibrosis), CAPN5 and CLN3 (neurodegeneration), and PRDM13 (transcriptional regulation). These proteins have previously been implicated in photoreceptor apoptosis, complement activation, and extracellular matrix remodeling—key processes in IRD progression. The model captured the transition between disease phases using pathway-level proteomic data, supporting the hypothesis of molecular thresholds driving phase shifts in retinal degeneration. The mutational burden model can be integrated into clinical diagnostic pipelines to reclassify patients who test negative under Mendelian criteria, improving genetic counseling and guiding inclusion in gene therapy programs. The proteomic classifier provides a novel tool for dynamic patient monitoring, identifying disease activity phases that may benefit from therapeutic intervention. Both approaches are scalable, data-driven, and suitable for translation into omics-based diagnostics. They can be deployed in biotechnological platforms for clinical decision support, biomarker discovery, and stratification in clinical trials targeting IRDs.

This study presents an integrated omics approach to address both the genetic and temporal complexity of inherited retinal dystrophies. By combining mutational burden analysis with machine-learning-based proteomic classification, we provide a framework capable of

reclassifying patients with unresolved genotypes and detecting clinically relevant shifts in disease progression. These tools contribute to a paradigm shift beyond Mendelian diagnostics, supporting the development of precision medicine strategies for retinal diseases. Future steps include validation in independent IRD cohorts using real-world proteomic and genomic data, functional characterization of novel gene combinations, and integration with imaging and clinical phenotypes.

CHAPTER 1 – INTRODUCTION

1.1 Inherited Retinal Dystrophies (IRDs)

Inherited Retinal Dystrophies (IRDs) are a diverse group of rare, genetically inherited disorders that primarily affect the photoreceptor cells and the retinal pigment epithelium (RPE), leading to progressive visual impairment and, ultimately, blindness. These diseases encompass a wide range of clinical entities, including retinitis pigmentosa (RP), Leber

congenital amaurosis (LCA), cone-rod dystrophy, Stargardt disease, and Usher syndrome. Although these disorders differ in their specific genetic causes, age of onset, and rates of progression, they share a common endpoint: the irreversible degeneration of photoreceptors and the disruption of the retinal architecture [1-3].

Epidemiological studies estimate the global prevalence of IRDs at approximately 1 in 3,000 individuals, which, when aggregated, makes them one of the most frequent causes of inherited blindness in the developed world. Clinically, patients may present with nyctalopia, peripheral field constriction, color vision defects, or loss of central vision, depending on the specific photoreceptor populations involved. The disease course is usually slowly progressive, yet the pace and pattern of deterioration can vary substantially between patients—even among those harboring identical pathogenic variants. This variability highlights the complexity of the molecular pathways related to retinal homeostasis and suggests that additional modifiers, both genetic and environmental, influence disease expression [4,5].

From a genetic perspective, IRDs exhibit extreme locus and allelic heterogeneity. More than 270 genes have been identified to date as causative, encompassing diverse biological processes such as phototransduction (*RHO, CNGB1, GNAT1*), visual cycle metabolism (*ABCA4, RPE65, RDH12*), ciliogenesis (*USH2A, CEP290, RPGR*), and synaptic transmission (*CACNA1F, CABP4*). Genetic variants in these genes can be transmitted through autosomal dominant (AD), autosomal recessive (AR), or X-linked modes of inheritance. However, several genes, such as *ABCA4* and PRPH2, are known to exhibit variable inheritance patterns depending on the nature of the variant and its interactions with other alleles or genes [6]. The genotype and phenotype in IRDs are further compounded by incomplete penetrance and variable expressivity. Also, the phenotypic manifestations may vary widely, considering the dynamic state of retinal molecular pathways [7]. This complexity challenges the traditional Mendelian model, which assumes a one-to-one association

between a single pathogenic variant and the resulting phenotype. For this reason, a considerable fraction of IRD patients remain without a definitive molecular diagnosis, prompting a reevaluation of disease causality frameworks [8].

1.2 Mendelian and Oligogenic Models

The complex nature of retinal dystrophies stems from multiple factors, among them locus heterogeneity. Proteins encoded by locus heterogeneity genes exhibit high interconnectivity within the human protein interaction network and tend to cluster together [9]. Up to 30% of cases of locus heterogeneity involve disease-causing proteins that are members of the same protein complex [10]. This clustering suggests that these genes participate in similar biological processes and pathways [9]. Network analysis of retinitis pigmentosa genes and their interacting partners has identified potential new disease candidates and provided insights into the disorder's etiopathology [8]. Understanding these protein-protein interactions and molecular pathways is crucial for elucidating the mechanisms underlying locus heterogeneity [8, 10]. Studying complex protein-protein interactions and molecular pathways could be an appropriate approach to examine the associations among genes involved in several disorders.

Traditional genetic testing for Mendelian inheritance in hereditary retinal dystrophies has shown limitations in accurately diagnosing the diverse forms of these conditions. Recently, it has become evident that additional modes of inheritance, beyond the classic Mendelian framework, may contribute to retinal diseases. Indeed, retinal dystrophies can also result from interactions among single-allele variants across multiple genes, such as in digenic, trigenic, and oligogenic inheritance [7, 11]. Digenic inheritance, in which two genes are involved in disease, trigenic inheritance involving three genes, and oligogenic inheritance, indicating the influence of several genes, are examples of inheritance patterns that do not fit Mendelian inheritance but contribute to disease phenotypes [12, 13]. These concepts

bridge the gap between Mendelian and multifactorial traits, offering insights into how multiple genetic variations can converge to influence phenotypic outcomes. Oligogenic inheritance can affect not only retinal dystrophies but also related syndromes such as Usher syndrome (type ID), Usher syndrome (type IIC), Joubert syndrome 9, Joubert syndrome 15, Methylmalonic aciduria and homocystinuria, cblC type, and Bardet-Biedl syndrome **(Table 1)** [14-21].

Oligogenic diseases have been studied using a mutational burden model to identify potential genetic causes [22]. The Digenic Diseases Database (DIDA) contains information on 44 digenic diseases, comprising 213 digenic combinations, and defines a digenic combination as a set of variants in two distinct genes that together cause the patient's phenotype [23]. In a study of 124 digenic combinations from DIDA, 69% of the combinations had heterozygous variants in both genes. Of these heterozygous cases, 31% were true digenic cases, meaning that both genes were required for the development of the disease. The remaining 69% were composite cases, in which a variant in one gene was sufficient to produce the phenotype, but an additional variant in a second gene altered the disease phenotype or the age of onset, a phenomenon called epistasis [23]. Another study used a mutational burden model to identify digenic interactions in human diseases and developed the Digenic Interaction Effect Predictor (DIEP). DIEP is a machine-learning approach that achieved high accuracy and sensitivity in independent testing datasets, outperforming another gene-level digenic predictor. DIEP was able to discriminate between digenic interaction effects and bi-locus effects and demonstrated enrichment of digenic interactions in genome-wide pathogenic coding gene pairs [24]. Finally, mutational burden has been proposed to affect many genetic diseases, suggesting that the combined impact of rare genetic variants influences disease phenotype and contributes to clinical variability [25, 26].

The complexity of retinal dystrophies, stemming from the complex genetic landscape, variable symptoms, and diverse inheritance patterns, underscores the need for new

diagnostic methods. Patients with genetic disorders can exhibit various variants in single alleles of different recessive genes, leading to the production of altered proteins that may contribute to the disorder's manifestation [27]. The proteins produced by these mutated genes often interact within the same biochemical pathway, complicating the diagnostic process [28-30]. The presence of multiple variants in a single pathway can create a complex interplay of genetic and environmental factors that influence the severity and presentation of the disorder [31]. Advanced computational approaches, such as machine learning, are becoming increasingly crucial tools in analyzing complex genetic data and predicting disease outcomes and could be used to analyze the complex interplay among genes, gene-protein interactions, and protein-protein interactions [24]. Applying the Mendelian inheritance model yields negative diagnostic results in a substantial proportion of cases, ranging from 25% to 40% [32, 33]. We hypothesize that a subset of the negative results for the Mendelian inheritance model may test positive, considering other models of inheritance.

1.3 Molecular Pathways, Proteomics, and Phases of IRDs

Several genes responsible for IRDs have been identified; however, the clinical course can still be influenced by environmental and metabolic factors, including light exposure, chronic inflammation, oxidative stress, latent viral infections, excessive caloric intake, and micronutrient deficiencies [34, 35].

The clinical variability of IRDs is exemplified by phenotypic differences observed in patients with CNGA1 and CNGB1 mutations, in which earlier and more severe macular atrophy is often seen in *CNGB1*-related disease [36]. Likewise, *CRB1* mutations can manifest as a spectrum ranging from classic retinitis pigmentosa to severe early-onset Leber congenital amaurosis [37, 38].

Photoreceptor degeneration in individuals with *ABCA4* mutations is accelerated by exposure to high-energy blue light, which promotes the accumulation of toxic retinal byproducts [39, 40]. Also, chronic neuroinflammation—sustained by persistent activation of the complement cascade—exacerbates retinal damage and contributes to disease progression [41]. Genetically, truncating mutations typically result in a complete loss of protein function, often correlating with early onset and more aggressive phenotypes. In contrast, missense variants cause partial functional deficits that cumulatively induce cellular stress, eventually exceeding the retina's compensatory capacity and triggering degeneration once a threshold is crossed [42-44].

IRDs follow a non-linear progression, marked by alternating latent and active phases driven by molecular thresholds that govern retinal homeostasis. In this framework, disease onset typically begins with a latent phase initiated by genetic defects or environmental stressors. During this stage, photoreceptors remain functionally preserved due to the activation of compensatory pathways [45-48]. The retina activates protective mechanisms, including the release of neurotrophic factors such as BDNF and CNTF, which support photoreceptor viability and Müller cell function. [49, 50] Concurrently, metabolic adaptations—including enhanced angiogenesis and upregulated fatty acid oxidation—serve to meet the retina's high energetic demands, particularly in the context of chronic hypoxia. As these mechanisms gradually lose efficacy under persistent stress, the system enters an active phase characterized by accelerated degeneration [51, 52].

An additional protective mechanism involves upregulating molecular chaperones, such as BiP and GRP94, which alleviate endoplasmic reticulum stress by facilitating proper protein folding and limiting the accumulation of misfolded proteins [53-54]. Despite these compensatory pathways, subclinical damage accumulates during the latent phase. A key driver of the transition to degeneration is mitochondrial stress, which disrupts the electron transport chain and results in excessive reactive oxygen species production [55, 56].

Early indicators of metabolic stress can be detected through non-invasive imaging techniques. Retinal autofluorescence, for instance, reveals toxic bisretinoid accumulation—often asymptomatic initially—that reflects underlying oxidative burden. In patients with *ABCA4* mutations, impaired visual cycle clearance leads to a pathological buildup of A2E in the RPE, exacerbating oxidative damage and reducing antioxidant defenses. This process follows a biphasic trajectory: an initial phase of gradual autofluorescent material deposition with preserved visual function, followed by a second phase marked by blood-retinal barrier disruption. The onset of cystoid macular edema or choroidal neovascularization during this stage is associated with rapid visual decline [57, 58].

Recent findings indicate that mitochondrial stress responses are tightly regulated by microRNAs, particularly miR-181a/b, which play a crucial role in photoreceptor survival. Inhibition of these microRNAs in murine models has been shown to attenuate apoptosis, suggesting that crossing a critical mitochondrial stress threshold may be sufficient to trigger irreversible neurodegeneration [59].

Inflammation plays a central role in the progression of IRDs, particularly during the transition to the active degenerative phase. Activation of the complement cascade—primarily through C3a and C5a—amplifies retinal injury and contributes to neuronal loss [60-62]. Experimental evidence indicates that pharmacological inhibition of complement components can attenuate tissue damage during active disease phases, supporting their therapeutic relevance [63]. In parallel, the depletion of antioxidant defenses during this stage leads to the accumulation of reactive oxygen species, initiating apoptotic pathways that further compromise photoreceptor integrity [64]. Additionally, the accumulation of lipofuscin in the RPE induces the release of pro-inflammatory cytokines, such as IL-1β and TNF-α, further destabilizing the blood-retinal barrier and facilitating the shift toward the active phase. Concurrently, retinal microglia become strongly activated, secreting inflammatory mediators that intensify neuroinflammation and hasten neuronal degeneration [65, 66].

Plasma proteomics is a valuable tool for complementing genetic diagnostics in IRDs by identifying molecular signatures associated with early neurodegeneration, inflammation, and vascular dysfunction [67-70]. In patients with *CRB1* mutations, elevated plasma levels of Complement Factor H and CFHR2 suggest chronic complement activation linked to accelerated photoreceptor loss [71]. Increased neurofilament light chain (NfL) correlates with axonal damage and visual field constriction, while truncated rhodopsin fragments in individuals with *RHO-P23H* mutations indicate ongoing rod degeneration [72].

Similar profiles are observed in age-related macular degeneration (AMD), where elevated CFH and Complement Factor B levels predict neovascular risk, particularly in carriers of the Y402H polymorphism [73]. In geographic atrophy, membrane attack complex accumulation reflects sustained inflammation, with increased fibulin-3 and TIMP-3 predicting lesion progression. A VEGF/PEDF ratio above 13 has been shown to anticipate neovascular membrane formation months in advance. Integration of APOE, C3a, and MMP-9 improves the prediction of AMD progression, reaching 89% accuracy [74].

To capture the non-linear dynamics of IRDs, several mathematical models have been developed [75, 76]. In retinitis pigmentosa, partial differential equation models incorporating oxygen diffusion and cell density have demonstrated how rod loss induces hyperoxia, driving damage propagation via toxic gradients [75]. Other models using ordinary differential equations and Hill kinetics have shown that metabolic coupling between glycolysis and oxidative stress in cones can produce bistable states, explaining abrupt degeneration [76]. Experimental work in murine models has confirmed these dynamics, identifying a conserved pattern of latent compensation followed by rapid photoreceptor loss, linked to sequential activation of apoptotic pathways [77]. These findings reinforce the importance of dynamic biomarkers for real-time disease phase classification.

1.4 Aim of the Project

This project aims to address two critical challenges in the diagnosis and clinical stratification of Inherited Retinal Dystrophies (IRDs): the genetic resolution of Mendelian-negative cases and the dynamic characterization of disease progression.

First, we aim to determine whether individuals lacking a definitive genetic diagnosis exhibit a statistically significant accumulation of rare, heterozygous variants in genes involved in retinal function. We hypothesize that such mutational accumulation—when distributed across functionally related pathways—may underlie pathogenic mechanisms consistent with oligogenic inheritance. To test this, we developed a quantitative model of mutational burden. By mapping these variants to curated biological pathways, we assessed their enrichment in unsolved IRD cases relative to controls. Furthermore, we sought to identify gene combinations recurrently found in patients, but absent in controls, which may represent novel oligogenic signatures with potential diagnostic relevance.

Second, we aim to model the non-linear behavior of IRDs by developing a machine learning–based classifier capable of distinguishing between active and latent disease phases using plasma proteomic data. Given that IRD progression involves discrete molecular transitions not captured by static genetic data, there is a pressing need for biomarkers that reflect dynamic biological states. Our approach uses protein expression profiles associated with ten key biological domains—inflammation, oxidative stress, immune response, apoptosis, aging, visual perception, ciliopathies, lipid metabolism, cellular transport, and intracellular signaling—to generate a classification model.

Together, these complementary models aim to improve the diagnostic yield of IRDs studying oligogenic patterns of inheritance in unresolved cases and provide a model for disease monitoring based on proteomic phase classification.

CHAPTER 2 – MATERIALS AND METHODS

2.1 Mutational Burden Model

2.1.1 Data Collection

A dataset was constructed retrospectively analyzing demographic data, genetic data, and specific ophthalmologic data collected by clinical specialists for hereditary degenerative disease. The dataset includes patients who were referred as negative for Mendelian genetic testing but have symptoms similar to an inherited retinopathy; indeed, their visual field is very limited. These patients were referred to as “Unhealthy patients”. Another dataset of patients diagnosed with other genetic diseases was included as “Control patients”. The datasets include, anonymously coded, information such as age, genetic variants, nucleotide, amino acid, “ACMG classifications”, VF (Visual Field) in the right eye, VF in the left eye, and mean VF. Genetic variants have been classified according to the ACMG guidelines as pathogenic, likely pathogenic, and variant unknown significance (VUS HOT) [78].

The patients were informed about the significance of genetic testing, and we obtained written informed consent from all of them, in accordance with the Declaration of Helsinki. Ethical

approval and clearance were received from the Ethical Committee of Azienda Sanitaria dell' Alto Adige, Italy (Approval No. 132-2020).

2.1.2 Data processing and data transformation

For each ACMG interpretation, we assigned a value based on the effect of the variant with respect to the phenotype. Therefore, we assumed a variant classified as “Pathogenic” or “Likely Pathogenic” to have a higher role in the possible occurrence of the disease than a “VUS”. ACMG classifications were assigned weights based on their pathogenicity levels (P = 0.5, LP = 0.3, VUS HOT = 0.2) and normalized by age to account for potential age-related biases. The data processing pipeline was designed to normalize the “Pathogenicity weight”, assigned to each variant, by patient age, map mutated genes to metabolic pathways, and perform statistical comparisons between patient and control groups. The overall workflow is summarized in **Figure 1**. Normalized “Pathogenicity weight” were integrated into the dataset, which included patient ID, mutated gene, ACMG classification, mean clinical evaluations of the eyes (VF Mean), and date of birth. This normalization step ensured that the impact of age on genetic evaluation was minimized before further analysis. Clinical data of control patients were missing for VF. These individuals were not diagnosed for any retinal diseases; therefore, we assumed that the VF of these individuals was 10. In the “unhealthy patients” group, missing VF values were imputed with random values ranging from 1 to 7. Given these last steps, the datasets were considered semi-synthetic.

A dictionary was constructed to map genes to their corresponding metabolic pathways using publicly available databases, including KEGG and Reactome, as well as STRING, an open-source tool used to retrieve enriched pathway information for genes with at least one variant in the dataset (**Table 2**). Mutated genes identified in the “unhealthy patients” group were systematically mapped to these metabolic pathways to enable detailed pathway enrichment

analysis. Dummy columns were added to the main dataframe to represent the mutated genes and their associated pathways, facilitating downstream calculations.

Once “Pathogenicity weight” was normalized, they were multiplied by the corresponding values in the metabolic pathway columns to calculate a weighted score that represented the contribution of each gene to its associated pathways. The data were then grouped by patient ID, with the pathway scores and “Pathogenicity weight” aggregated by summing the metabolic pathway data and averaging the “Pathogenicity weight”. This step provided a consolidated view of each patient’s genetic and pathway-level data. Mean values for each metabolic pathway were also calculated separately for the interest group (patients with retinal dystrophies) and the control group. Finally, a Mann-Whitney U test was performed to compare the metabolic pathway scores between the interest group and the control group. This non-parametric test was chosen to account for the non-normal distribution of the data, enabling robust statistical comparisons of the mean values across pathways. The results of this analysis highlighted pathways with significant differences between the two groups, shedding light on the potential role of metabolic pathways in the disease mechanism.

2.1.3 Statistical Analysis

Statistical analyses were performed using the Mann-Whitney U test and the Shapiro-Wilk test for normality to evaluate data distributions, correlations, and significance levels. The Mann-Whitney U test was applied to assess differences between gender and key variables, including MEDIA LE+RE (LE: left eye; RE: right eye), mutated gene counts, and age. Correlation analysis was conducted to examine relationships between variables, with correlation heatmaps constructed to visualize the dataset's interactions. Python libraries like Pandas, NumPy, Seaborn and scikit-learn were used to perform statistical analysis on the dataset and for data visualization. Data were considered to be statistically significant when p value was lower than 0.05.

2.1.4 Probabilistic Kernel Density Estimation

Kernel Density Estimation (KDE) was used to quantify the association between mutational burden and retinal conditions, specifically focusing on a single pathway. To ensure comparability across the cohorts, feature values were standardized to have a mean of zero and a standard deviation of one. To determine the optimal smoothness of the KDE model, a rigorous cross-validated grid search was conducted to pinpoint the best bandwidth parameter. With the optimal bandwidth identified, the KDE model was fitted to the standardized feature values, and a comprehensive evaluation of the density across a range of values was performed. A key component of the analysis involved the calculation of percentile ranks for each patient's standardized feature value. A threshold at the 90th percentile was established, classify patients based on their mutational burden. Mutational burden is associated with the retinal condition in patients exhibiting higher feature values, surpassing the threshold.

2.2 Active/Latent Phase

2.2.1. Synthetic Dataset Generation

A synthetic dataset consisting of 500 samples was generated to simulate the plasma proteomic profiles of healthy individuals and patients affected by IRDs. Random gender and age values from 40 to 60 years were imputed for each sample. 315 proteins (**Table 3**) were selected based on their relevance to the molecular processes involved in retinal degeneration [https://retnet.org/]. Considering mass spectrometry data distribution [79, 80] and taking as an example the concentration of proteins in public databases (https://www.proteinatlas.org/), protein concentration levels were imputed with arbitrary

values. Normalization was performed using MinMax scaling, transforming protein expression values into a range between 0 and 1 to ensure data uniformity.

2.2.2 Protein Classification in Biological Pathways

To select the most representative proteins, only those with an expression frequency equal to or greater than 50% in the samples were considered for the further steps of the analysis. The selected proteins were categorized into ten major biological pathways associated with the pathogenesis of retinal dystrophies based on literature and database search: inflammation, oxidative stress, immunity, apoptosis, aging, visual perception, ciliopathies, lipid metabolism, cellular transport, and signal transduction. For each sample, a pathway score was calculated as the weighted average of the expression levels of the proteins belonging to each pathway, allowing the functional analysis of the synthetic proteomic profiles.

2.2.3 Patients Classification in Active/Latent Phase

The samples were classified as belonging to the active or latent phase of the disease based on the level of activation of biological pathways. Pathways with a normalized score equal to or greater than the arbitrary value 0.70 were considered "active," while those with values below this threshold were defined as "latent." Samples with at least two activated pathways (score ≥0.70) were classified as being in the active phase of the disease, while those with all pathways in a latent state or only one activated pathway were assigned to the latent phase.

2.2.4 Machine Learning Model

To classify the samples into the active or latent phase, a machine learning model was implemented using Python. The final dataset was divided into a training set (80%) and a test set (20%) for model validation. Before training, the data were rescaled using MinMaxScaler to ensure uniform numerical scaling of the variables. Four ML algorithms were tested: Support Vector Machine (SVM), Random Forest (RF), Logistic Regression (LR), and Extreme Gradient Boosting (XGBoost). The selection of the best model was performed by comparing standard performance metrics, including accuracy, precision, recall, and F1-score, with parameters optimized through cross-validation techniques. The analysis of variable importance was conducted by evaluating the coefficients of the ML model with the best performance metrics, identifying the proteins with the greatest contribution to sample classification. This procedure allowed for the selection of the most relevant protein biomarkers for patient stratification and the interpretation of molecular mechanisms involved in the progression of hereditary retinal dystrophies.

CHAPTER 3 – RESULTS

3.1 Mutational Burden Model

3.1.1 Clinical Data

The cohort is composed of 527 patients divided into “unhealthy patients” and control patients, with the clinical data reported in **Table 4**. The “unhealthy patients” group includes 453 individuals, while the control patients group consists of 74 individuals. Among the unhealthy patients, 53% were males and 47% females, compared to the “control patients” group that was composed of 69% males and 31% females. The age range of unhealthy patients spans from 11 to 102 years, with a mean age of 47 ± 19 years. The control patients have an age range from 8 to 86 years, with a mean age of 46 ± 20 years. Unhealthy patients showed a Mean LE+RE of 4.44 ± 1.38, whereas control patients exhibited a significantly higher score of 10 ± 0. This is in line with the creation criteria of the semi-synthetic dataset. The “Pathogenicity weight” score is higher in unhealthy patients (0.38 ± 0.13) compared to control patients (0.18 ± 0.03), indicating that, although control patients have a higher average number of mutated genes (4.96 ± 1.77 vs 2.52 ± 1.67), their variants are on average of low pathogenicity. The Mann-Whitney U test result indicated that there was no statistically significant difference between age distributions in the two groups ($p = 0.617$). The similar age distributions between the control and unhealthy groups suggest that age is not a confounding factor in the comparison of other variables, such as pathway activations and “Pathogenicity weight” scores. The chi-square test for independence result indicated that there was a statistically significant difference in the gender distribution between the control

and unhealthy groups. The higher proportion of males in the unhealthy group suggests a potential gender-related factor in the prevalence of retinal conditions, warranting further investigation [80, 81].

3.1.2 Pathway Enrichment, Mutational Burden Distribution, and Identification of Unique Gene Combinations in IRD Patients

The correlation analysis assessed the relationship among different molecular pathways. Several key pathways involved in photoreceptor function and retinal maintenance exhibited strong positive correlations, with Pearson correlation coefficients approaching 1.0. These findings suggest a high degree of functional connectivity among the genetic modules implicated in IRDs (**Table 5**). To identify pathways with significantly different activation levels between patients and controls, we performed a Mann–Whitney U test. The results, displayed in **Figure 2** as a scatter plot of p-values on a logarithmic scale, allowed us to prioritize pathways based on statistical relevance. The two most significantly enriched pathways in the patient group were “The Canonical Retinoid Cycle in Rods” (Twilight Vision) ($p = 0.012084$) and “Retinoid Cycle Disease Events” ($p = 0.00002$), highlighted in red. Additional pathways, including those related to visual phototransduction, sensory perception, and retinal homeostasis, also showed notable differences, indicated in blue.

To further characterize the distribution of mutational burden across individuals, we applied KDE, focusing on “The Canonical Retinoid Cycle in Rods” (Twilight Vision) pathway due to its statistical significance and strong correlation with the “Retinoid Cycle Disease Events” pathway. The establishment of a 90th percentile threshold facilitated the classification of patients. KDE allowed for non-parametric estimation of the distribution of pathway-specific burden values. **Figures 3A** and **3B** illustrate this distribution, with the KDE curve depicting density and a vertical dashed line marking the high-burden cutoff. Peaks in the KDE curve

denote subgroups of patients sharing similar mutational profiles, improving the interpretability of burden stratification.

In addition to quantifying mutational burden, we examined whether specific gene combinations within the twilight vision pathway were uniquely present in affected individuals. Given the overlapping gene content and high correlation between the two most significant pathways, we focused our analysis on the twilight vision pathway. We first selected all individuals carrying at least one variant in any gene within this pathway, identifying 207 patients and 27 controls. We then enumerated all possible gene pair combinations within this subset and filtered for those exclusively observed in the patient group. Two gene pairs—(*ABCA4, RDH12*) and (*ABCA4, RBP3*)—were found only in the affected cohort (**Figure 4**). Although Fisher's exact test did not show a statistically significant difference in the frequency of these combinations between patients and controls (**Table 6**), their exclusive presence in the disease group, coupled with their biological relevance, supports their candidacy as potential oligogenic contributors, warranting further functional validation.

3.2 Active/Latent Phase

3.2.1 Proteomic Panel and Phase Classification of Synthetic IRD Samples

The synthetic proteomic dataset comprised expression profiles for 315 proteins implicated in retinal dystrophies. **Table 7** summarizes the expression frequency, mean intensity, and standard deviation of the most represented proteins across the 500 simulated samples. As shown in **Figure 5**, the dataset exhibited substantial heterogeneity in protein expression. Proteins such as CAPN5, CLN3, NDP, and TIMP3 showed high inter-sample variability, suggesting dynamic regulation consistent with disease phase transitions. Conversely, proteins like ABCC6, AFG3L2, and CFB exhibited relatively low and stable expression across the dataset. To contextualize the proteomic signals within relevant biological

processes, the top 82 most consistently expressed proteins (≥50% expression frequency) were annotated to ten retinal disease-associated pathways: inflammation, oxidative stress, immune response, apoptosis, aging, visual perception, ciliopathies, lipid metabolism, cellular transport, and signal transduction (**Table 8**).

For each sample, a pathway activation score was calculated by averaging the normalized expression levels of the proteins associated with each pathway. Based on these scores, samples were categorized into two groups: active phase (≥2 pathways with scores ≥0.70) and latent phase (all pathways below threshold or only one active). Using this classification strategy, 262 samples were assigned to the active phase, while 238 were labeled as the latent phase, reflecting a balanced distribution suitable for machine learning analysis.

3.2.2 Machine Learning Classification of IRD Disease Phases

To assess the capacity of proteomic data to discriminate between active and latent phases of inherited retinal dystrophies, four machine learning algorithms—Logistic Regression (LR), Support Vector Machine (SVM), Random Forest (RF), and XGBoost—were trained and evaluated on the synthetic dataset. Model performance was assessed using standard classification metrics: accuracy, precision, recall, and F1-score. As reported in **Table 9**, Logistic Regression outperformed the other models, achieving an accuracy of 72%, a precision of 0.72, and an F1-score of 0.71. XGBoost and SVM followed closely with accuracies of 70% and 69%, respectively. The Random Forest model exhibited the lowest performance, with an accuracy of 64%.

To further evaluate the classification behavior of the best-performing model (Logistic Regression), a confusion matrix was generated on the test set of 100 samples (**Figure 6**). The model correctly identified 43 active-phase and 29 latent-phase cases. However, 16 samples were incorrectly classified as active-phase (false positives), and 12 were misclassified as latent-phase (false negatives). This distribution highlights a slightly higher

sensitivity toward detecting the active phase but also underscores areas for future optimization. Also, we investigated the feature importance within the Logistic Regression model to determine which proteins most strongly contributed to phase discrimination (**Figure 7**). The analysis revealed TIMP3, VEGFA, PRDM13, CAPN5, and CLN3 as the most influential biomarkers. These proteins are known to be involved in key retinal processes, including extracellular matrix remodeling, angiogenesis, transcriptional regulation, and neurodegeneration—supporting their potential as dynamic indicators of IRD progression.

CHAPTER 4 – DISCUSSIONS

IRDs represent a heterogeneous group of monogenic disorders characterized by progressive dysfunction and degeneration of photoreceptors, leading to irreversible vision loss [1-3]. Although the advent of NGS technologies—including targeted panels and exome sequencing—has substantially improved diagnostic yield, a significant proportion of patients remain genetically unsolved when interpreted under traditional Mendelian paradigms. This diagnostic gap underscores the need to explore alternative models of inheritance that better capture the complexity of retinal diseases [9].

Building on emerging evidence that rare variant accumulation across functionally interconnected genes may drive disease phenotypes [25-26], we developed a model to quantify mutational burden in IRDs. This approach integrates systems biology with mathematical modeling to assess whether the cumulative effect of multiple rare heterozygous variants in biologically related pathways contributes to disease expression in Mendelian-negative individuals. Using curated IRD gene sets and pathway mappings from KEGG, Reactome, and STRING, we constructed a mutational burden model applied to semi-synthetic clinical datasets comprising genetically unsolved IRD cases and unrelated controls. For the model development, two semi-synthetic datasets were used, each reporting clinical and genetic data of patients affected by retinal dystrophies (“Unhealthy patients”) or patients affected by other genetic diseases (“Control patients”). The model tries to assess the cumulative impact of genetic variants within the selected genes and the identified molecular pathways.

Statistical comparison between groups showed two pathways with the most significant burden enrichment: “The Canonical Retinoid Cycle in Rods” (Twilight Vision) ($p = 0.0121$) and “Retinoid Cycle Disease Events” ($p = 0.00002$). These pathways show the robust activation in the patient group, and they were also highly correlated ($r = 0.92$), suggesting shared mechanisms for photoreceptor maintenance and visual cycle metabolism. To delineate individuals with exceptionally high mutational loads, KDE was used to model the

distribution of burden scores. A threshold set at the 90th percentile was used to stratify patients, defining a high-burden subgroup potentially at risk due to cumulative oligogenic effects.

One of the central challenges in clinical genomics is the interpretation of variants that lie outside the explanatory power of single-gene Mendelian inheritance [83, 84]. Our results support growing research in systems biology and genomics, indicating that variants in different genes—particularly those participating in the same molecular pathways—can interact synergistically to produce disease phenotypes. This paradigm shift recognizes the retina not as a collection of isolated gene functions, but as an integrated molecular system governed by thresholds, redundancy, and interaction dynamics [85, 86].

The mutational burden framework enabled the identification of gene pairs exclusive to the patient group but absent in controls— (*ABCA4, RDH12*) and (*ABCA4, RBP3*). While statistical significance was not reached due to sample size, the recurrence of *ABCA4*, a well-characterized gene associated with Stargardt disease and cone-rod dystrophy, in previous studies has demonstrated its oligogenic interactions with *ROM1, PRPH2, and PROM1* [86-88].

The identification of new oligogenic signatures offers a promising strategy for reclassifying unsolved IRD cases. However, several limitations must be acknowledged. The model relies on the accuracy and completeness of existing protein–protein interaction networks and gene–pathway annotations, which may be subject to knowledge biases and database limitations [84, 89, 90]. Additionally, the datasets used were semi-synthetic, which, while controlled and standardized, may not capture the full spectrum of interindividual genetic variation seen in real cohorts. Furthermore, retinal dystrophies are phenotypically and genetically diverse, with variable expressivity and incomplete penetrance that can obscure genotype–phenotype relationships. Functional studies and independent studies should validate the results obtained [84, 89].

Despite these limitations, our results align with recent studies that used machine learning and network-based modeling to study complex genetic datasets [25]. In summary, our approach contributes to a broader effort to contribute to genetic diagnostics in IRDs by moving beyond Mendelian constraints. If validated in larger and independent cohorts, the mutational burden model could offer a powerful tool to discover novel oligogenic patterns, refining molecular diagnoses, and improving personalized treatment strategies in retinal disease. This work reinforces the principle that genotype interpretation must increasingly consider the interplay of multiple rare variants within biologically coherent networks, paving the way for new approaches to clinical genomics.

IRDs follow a non-linear course marked by alternating latent and active phases, driven by molecular thresholds regulating retinal homeostasis. This degeneration involves episodic photoreceptor stress, cellular remodeling, and inflammation [45, 46]. During the latent phase, visual function is maintained through compensatory mechanisms despite underlying mitochondrial and inflammatory stress [47, 48]. As oxidative and metabolic damage accumulates, critical thresholds are crossed, triggering the active phase with complement activation, apoptosis, and irreversible photoreceptor loss [63, 64]. Timely identification of the transition from latent to active phase represents a major clinical challenge, especially in the context of treatment stratification and early intervention. To address this, we developed a classification model trained on a synthetic proteomic dataset that simulates protein expression dynamics across key biological pathways implicated in IRDs. While the absence of a real cohort limits clinical translation at this stage, the model provides a proof-of-concept for leveraging pathway-level protein profiles to discriminate disease phases based on molecular activity. Classification was driven by a systems-level interpretation of ten key retinal pathways, with samples categorized as "active" if two or more pathways showed elevated activation scores. This approach mirrors the complex nature of retinal degeneration, where simultaneous dysregulation of oxidative stress, inflammation,

apoptosis, and visual transduction networks underlies clinical progression. The resulting classifier achieved robust discrimination between simulated active and latent profiles, despite the artificial nature of the dataset, and generated biologically plausible outputs.

From a biomarker discovery perspective, feature importance analysis highlighted proteins most influential in classifying IRD disease phases. In our synthetic dataset, TIMP3, VEGFA, PRDM13, CAPN5, and CLN3 emerged as key contributors—pointing to roles in extracellular matrix remodeling, vascular permeability, and neurodegeneration [91-95]. These findings align with prior evidence linking TIMP3 and VEGFA to retinal fibrosis and neovascularization [91, 92] and implicating CLN3 and CAPN5 in calpain-mediated neurodegeneration [93-95]. Although based on simulated data, the model demonstrates the potential of proteomic-based computational approaches for identifying phase-specific biomarkers. However, as a proof of concept, it requires validation on real cohorts and datasets to confirm its clinical relevance and ability to accurately distinguish between latent and active disease stages.

Both models provide a comprehensive framework that captures both the genetic complexity and the dynamic molecular behavior of IRDs, offering an integrated systems-level perspective that could advance diagnostic interpretation.

CHAPTER 5 – INDUSTRIAL APPLICATION

The two developed models—the mutational burden model and the proteomic-based phase classifier—offer distinct yet complementary industrial and clinical applications.

The mutational burden model provides a novel framework for extending the diagnostic capability of existing NGS pipelines. Quantifying the cumulative effect of rare variants across functionally related pathways enables the reclassification of Mendelian-negative patients and identifies potential oligogenic gene interactions. This model can be incorporated into bioinformatics platforms as an advanced interpretation module, improving diagnostic

accuracy and supporting patient selection for gene and cell therapy programs. For the industry, it offers a scalable computational tool that enhances variant prioritization and facilitates target discovery in multi-gene therapeutic approaches.

The proteomic-based model, trained to distinguish latent and active disease phases, provides a proof-of-concept for dynamic patient monitoring based on molecular activity rather than clinical endpoints. Once validated on real-world proteomic data, this approach could evolve into a companion screening or diagnostic tool for tracking therapeutic response, optimizing treatment timing, and stratifying patients in clinical trials. The identification of key biomarkers such as TIMP3, VEGFA, CAPN5, and CLN3 supports the potential development of commercial assays or biosensor platforms for disease activity monitoring.

From a patient care perspective, these models pave the way for personalized, predictive, and preventive ophthalmology. Integrating genomic and proteomic information enables clinicians to anticipate disease progression, intervene earlier, and tailor therapies to individual molecular profiles. Industrial validation and regulatory approval of these tools could lead to their integration in diagnostic laboratories and specialized retinal centers, transforming IRD management from descriptive to data-driven precision medicine.

CHAPTER 6 – CONCLUSIONS

IRDs represent one of the most genetically heterogeneous groups of monogenic disorders, and yet a significant portion of patients remain unsolved under traditional Mendelian diagnostic frameworks. Concurrently, the clinical course of IRDs is non-linear, marked by alternating latent and active phases that cannot be fully captured by static genomic data. These two limitations—genetic diagnostic incompleteness and lack of dynamic disease monitoring—form the foundation of the present study.

To address the first challenge, we developed a mutational burden model capable of quantifying the cumulative effect of rare heterozygous variants across functionally related genes. By integrating pathway-based annotation with pathogenicity scoring and KDE, we stratified patients based on their overall genetic burden. The model identified two

significantly enriched visual cycle pathways and gene combinations exclusive to IRD patients— (*ABCA4, RDH12*) and (*ABCA4, RBP3*)—suggesting a potential oligogenic basis in a subset of Mendelian-negative cases. Although these findings require validation in real cohorts, they demonstrate how systems biology and mathematical modeling can reveal hidden layers of genetic causality and aid in reclassifying previously unsolved patients.

To address the second challenge, we developed a proteomic phase classifier using synthetic plasma data and supervised machine learning. The model accurately distinguished between latent and active disease phases based on pathway-level protein expression, identifying key biomarkers such as TIMP3, VEGFA, CAPN5, and CLN3. These proteins are implicated in inflammation, neurodegeneration, and extracellular matrix remodeling, core processes in IRD progression. Despite the synthetic nature of the dataset, the classifier generated biologically plausible outputs and provides a preliminary model for developing dynamic tools to monitor disease activity and guide clinical decision-making.

Taken together, the two models offer a complementary framework that addresses both the static genetic architecture and the dynamic molecular behavior of IRDs. The mutational burden model improves diagnostic yield by identifying oligogenic contributors, while the proteomic classifier supports real-time stratification and potential treatment monitoring. Both approaches reflect a shift from monogenic and phenotype-based reasoning to a network-based, multi-omic paradigm that is increasingly necessary in complex rare diseases.

From a translational perspective, these tools have potential industrial and clinical applications. The genetic model could enhance variant interpretation pipelines in commercial diagnostics, inform gene therapy eligibility, and prioritize targets for functional validation. The proteomic model could evolve into a biomarker-based monitoring system, assisting clinicians in determining when to intervene and how to stratify patients for precision treatments.

Despite their promise, the current models are limited by their use of semi-synthetic datasets and require validation on real patient data. Future work should focus on applying these methods to large, multi-ethnic IRD cohorts, integrating genomic, proteomic, imaging, and clinical variables. Functional studies will be essential to confirm the pathogenicity of novel gene combinations and to validate phase-specific biomarkers. Moreover, expanding these models to incorporate transcriptomic or metabolomic data could offer a more comprehensive view of IRD pathophysiology.

In conclusion, this study demonstrates the feasibility and utility of multi-omic, computational approaches in advancing the diagnosis, monitoring, and understanding of inherited retinal dystrophies. By bridging gaps in genetic resolution and disease phase detection, it contributes to the foundation for precision ophthalmology, ultimately aiming to improve patient care and accelerate therapeutic development in the field of retinal genetics.

TABLES

TABLE 1. Digenic and Oligogenic Diseases Affecting Retina and Vision. This table presents examples of digenic and oligogenic diseases that impact retinal function and vision. It includes the disease name, OMIM number, associated genes, mode of inheritance, and relevant references.

Disease	OMIM	Genes	Inheritance
Retinitis pigmentosa 7	608133	*ROM1-RDS*	Digenic
Retinitis pigmentosa	-	*RP1L1-C2orf71*	Digenic
Usher syndrome, type ID	601067	*PCDH15-CDH23*	Digenic
Usher syndrome, type IIC	605472	*ADGRV1-PDZD7*	Digenic
Joubert syndrome 9	612285	*CC2D2A-CEP41*	Digenic
Joubert syndrome 15	614464	*CC2D2A-CEP41*	Digenic
Methylmalonic aciduria and homocystinuria, cblC type	277400	*MMACHC-PRDX1*	Digenic
Barde-Biedl Syndrome	-	*BBS1-BBS2-BBS4-BBS5-*	Oligogenic

		BBS6-BBS7-BBS9-APOE-C8orf37-CEP290-DNAAF1-ESR1-GHR-GUCY2C-MC4R-MCHR1-MKS1-NCOA2-NPC1-PDX1-RYR1-STRA6-ZNF423	
Familial exudative vitreoretinopathy	-	*FZD4-LRP5*	Digenic

TABLE 2. List of analyzed pathways and involved genes for each pathway.

Pathways	Genes
Activation of the phototransduction cascade	*CNGB1, PDE6A, RHO, CNGA1, PDE6B, SAG*
BBSome-mediated cargo-targeting to cilium	*BBS2, BBS10, MKKS, BBS7, BBS4, TTC8, BBS1, BBS12*
The canonical retinoid cycle in rods (twilight vision)	*ABCA4, RHO, RLBP1, MYO7A, RBP3, RDH12, RPE65, LRAT*
Retinoid cycle disease events	*ABCA4, LRAT, RDH12, RLBP1*
Cargo trafficking to the periciliary membrane	*CNGB1, RHO, BBS2, BBS10, MKKS, BBS7, RP2, BBS4, TTC8, NPHP3, BBS1, BBS12*
Inactivation, recovery, and regulation of phototransduction	*CNGB1, PDE6A, RHO, CNGA1, PDE6B, GUCY2D, SAG, GUCA1B*
Visual phototransduction	*ABCA4, CNGB1, PDE6A, RHO, CNGA1, PDE6B, GUCY2D, RLBP1, MYO7A, SAG, RBP3, RDH12, RPE65, LRAT, GUCA1B*
Sensory processing of sound by outer hair cells of the cochlea	*USH1G, FSCN2, MYO7A, PCDH15, WHRN, CDH23*
Sensory processing of sound by inner hair cells of the cochlea	*USH1G, FSCN2, MYO7A, PCDH15, WHRN, CDH23*
Cilium Assembly	*CEP290, CNGB1, RHO, BBS2, BBS10, MKKS, BBS7, RP2, BBS4, TTC8, IFT140, NPHP3, ALMS1, BBS1, BBS12, IFT172, OFD1*

Sensory Perception	*ABCA4, USH1G, CNGB1, PDE6A, RHO, CNGA1, FSCN2, PDE6B, GUCY2D, RLBP1, MYO7A, PCDH15, SAG, RBP3, WHRN, RDH12, CDH23, RPE65, LRAT, GUCA1B*
Retinopathies	*PCARE, TOPORS, RPGRIP1, SPATA7, CEP290, RP1, CNGB1, CNGA1, BBS2, FAM161A, RAB28, BBS10, CRX, MKKS, BBS7, C8orf37, TULP1, RP2, RP1L1, BBS4, TTC8, IFT140, NPHP3, POC1B, TTLL5, ALMS1, BBS1, BBS12, IFT172, OFD1, ARL2BP*
Phototransduction	*CNGB1, PDE6A, RHO, CNGA1, PDE6B, GUCY2D, GUCA1B, SAG*
Eye Development	*BBS4, BBS7, CEP290, FSCN2, GRM6, IFT140, IFT172, IMPG2, MERTK, MYO7A, NR2E3, NRL, PDE6A, PDE6B, PROM1, PRPH2, RHO, ROM1, RP1, RP1L1, RPE65, RPGRIP1, RS1, TOPORS, TTC8, TTLL5, TULP1, USH1C, ZNF513*
Detection of light stimulus	*ABCA4, AIPL1, BEST1, CACNA1F, CNGB1, ELOVL4, EYS, GRM6, NR2E3, PDE6B, PRPH2, RGR, RHO, ROM1, RP1, RPE65, RS1, SAG, TULP1*
Detection of visible light	*ABCA4, AIPL1, BEST1, CACNA1F, CNGB1, ELOVL4, EYS, GRM6, PDE6B, PRPH2, RGR, RHO, ROM1, RP1, RPE65, RS1, SAG, TULP1*
Photoreceptor cell development	*BBS1, BBS4, C8orf37, CDHR1, CEP290, CNGB1, FSCN2, IFT140, MYO7A, NR2E3, NRL, PCARE, PRPH2, ROM1, RP1, RP1L1, RPGRIP1, TOPORS, TULP1, USH1C*
Photoreceptor cell differentiation	*BBS1, BBS4, C8orf37, CDHR1, CEP290, CNGB1, FSCN2, IFT140, MYO7A, NR2E3, NRL, PCARE, PROM1, PRPH2, ROM1, RP1, RP1L1, RPGRIP1, TOPORS, TTC8, TULP1, USH1C*
Photoreceptor cell maintenance	*ABCA4, ADGRV1, BBS1, BBS10, BBS12, BBS2, BBS4, CDH23, CDHR1, CLRN1, CNGB1, MKKS, NPHP3, PCDH15, PROM1, RDH12, RHO, RP1L1, SPATA7, TULP1, USH1C, USH1G, USH2A*
Retina homeostasis	*ABCA4, ADGRV1, AIPL1, BBS1, BBS10, BBS12, BBS2, BBS4, CDH23, CDH3, CDHR1, CLRN1, CNGB1, MKKS, NPHP3, PCDH15, POC1B, PROM1, RDH12, RHO, RP1L1, RPE65, SPATA7, TULP1, USH1C, USH1G, USH2A, WHRN*

Sensory perception	*ABCA4, ADGRV1, AIPL1, BBS1, BBS10, BBS2, BBS4, BBS7, BEST1, CACNA1F, CDH23, CDH3, CLRN1, CNGA1, CNGA3, CNGB1, CNGB3, CRX, EYS, FAM161A, FSCN2, GPR179, GRM6, GUCA1B, GUCY2D, HMCN1, IMPG1, IMPG2, LRAT, MKKS, MYO7A, NR2E3, NRL, NYX, PCARE, PCDH15, PDE6A, PDE6B, PDZD7, PRCD, PRPH2, RAX2, RBP3, RDH12, RGR, RHO, RIMS1, RLBP1, ROM1, RP1, RP1L1, RP2, RPE65, RPGR, RPGRIP1, RS1, SPATA7, TIMP3, TRPM1, TTC8, TULP1, USH1C, USH1G, USH2A, WHRN, ZNF513*
Visual perception	*ABCA4, ADGRV1, AIPL1, BBS1, BBS10, BBS2, BBS4, BBS7, BEST1, CACNA1F, CDH23, CDH3, CLRN1, CNGA1, CNGA3, CNGB1, CNGB3, CRX, EYS, FAM161A, FSCN2, GPR179, GRM6, GUCA1B, GUCY2D, HMCN1, IMPG1, IMPG2, LRAT, MKKS, MYO7A, NR2E3, NRL, NYX, PCARE, PCDH15, PDE6A, PDE6B, PRCD, PRPH2, RAX2, RBP3, RDH12, RGR, RHO, RIMS1, RLBP1, ROM1, RP1, RP1L1, RP2, RPE65, RPGR, RPGRIP1, RS1, SPATA7, TIMP3, TRPM1, TULP1, USH2A, ZNF513*
Sensory perception of light stimulus	*ABCA4, ADGRV1, AIPL1, BBS1, BBS10, BBS2, BBS4, BBS7, BEST1, CACNA1F, CDH23, CDH3, CLRN1, CNGA1, CNGA3, CNGB1, CNGB3, CRX, EYS, FAM161A, FSCN2, GPR179, GRM6, GUCA1B, GUCY2D, HMCN1, IMPG1, IMPG2, LRAT, MKKS, MYO7A, NR2E3, NRL, NYX, PCARE, PCDH15, PDE6A, PDE6B, PRCD, PRPH2, RAX2, RBP3, RDH12, RGR, RHO, RIMS1, RLBP1, ROM1, RP1, RP1L1, RP2, RPE65, RPGR, RPGRIP1, RS1, SPATA7, TIMP3, TRPM1, TULP1, USH1C, USH1G, USH2A, WHRN, ZNF513*

TABLE 3. Proteomic Panel

Protein	GeneCards Link
ABCA4	https://www.genecards.org/cgi-bin/carddisp.pl?gene=ABCA4
ABCC6	https://www.genecards.org/cgi-bin/carddisp.pl?gene=ABCC6
ABHD12	https://www.genecards.org/cgi-bin/carddisp.pl?gene=ABHD12

ACBD5	https://www.genecards.org/cgi-bin/carddisp.pl?gene=ACBD5
ACO2	https://www.genecards.org/cgi-bin/carddisp.pl?gene=ACO2
ADAMTS18	https://www.genecards.org/cgi-bin/carddisp.pl?gene=ADAMTS18
ADGRA3	https://www.genecards.org/cgi-bin/carddisp.pl?gene=ADGRA3
ADGRV1	https://www.genecards.org/cgi-bin/carddisp.pl?gene=ADGRV1
ADH1C	https://www.genecards.org/cgi-bin/carddisp.pl?gene=ADH1C
ADH7	https://www.genecards.org/cgi-bin/carddisp.pl?gene=ADH7
ADIPOR1	https://www.genecards.org/cgi-bin/carddisp.pl?gene=ADIPOR1
AFG3L2	https://www.genecards.org/cgi-bin/carddisp.pl?gene=AFG3L2
AGBL5	https://www.genecards.org/cgi-bin/carddisp.pl?gene=AGBL5
AHI1	https://www.genecards.org/cgi-bin/carddisp.pl?gene=AHI1
AHR	https://www.genecards.org/cgi-bin/carddisp.pl?gene=AHR
AIPL1	https://www.genecards.org/cgi-bin/carddisp.pl?gene=AIPL1
ALDH1A2	https://www.genecards.org/cgi-bin/carddisp.pl?gene=ALDH1A2
ALDH1A3	https://www.genecards.org/cgi-bin/carddisp.pl?gene=ALDH1A3
ALDH8A1	https://www.genecards.org/cgi-bin/carddisp.pl?gene=ALDH8A1
ALMS1	https://www.genecards.org/cgi-bin/carddisp.pl?gene=ALMS1
APC	https://www.genecards.org/cgi-bin/carddisp.pl?gene=APC
APOD	https://www.genecards.org/cgi-bin/carddisp.pl?gene=APOD
APOE	https://www.genecards.org/cgi-bin/carddisp.pl?gene=APOE
ARHGEF18	https://www.genecards.org/cgi-bin/carddisp.pl?gene=ARHGEF18
ARL2BP	https://www.genecards.org/cgi-bin/carddisp.pl?gene=ARL2BP
ARL3	https://www.genecards.org/cgi-bin/carddisp.pl?gene=ARL3
ARL6	https://www.genecards.org/cgi-bin/carddisp.pl?gene=ARL6
ARMS2	https://www.genecards.org/cgi-bin/carddisp.pl?gene=ARMS2
ARSG	https://www.genecards.org/cgi-bin/carddisp.pl?gene=ARSG
ASRGL1	https://www.genecards.org/cgi-bin/carddisp.pl?gene=ASRGL1
ATXN7	https://www.genecards.org/cgi-bin/carddisp.pl?gene=ATXN7
BBIP1	https://www.genecards.org/cgi-bin/carddisp.pl?gene=BBIP1
BBS1	https://www.genecards.org/cgi-bin/carddisp.pl?gene=BBS1
BBS10	https://www.genecards.org/cgi-bin/carddisp.pl?gene=BBS10
BBS12	https://www.genecards.org/cgi-bin/carddisp.pl?gene=BBS12
BBS2	https://www.genecards.org/cgi-bin/carddisp.pl?gene=BBS2
BBS4	https://www.genecards.org/cgi-bin/carddisp.pl?gene=BBS4
BBS5	https://www.genecards.org/cgi-bin/carddisp.pl?gene=BBS5
BBS7	https://www.genecards.org/cgi-bin/carddisp.pl?gene=BBS7
BBS9	https://www.genecards.org/cgi-bin/carddisp.pl?gene=BBS9
BEST1	https://www.genecards.org/cgi-bin/carddisp.pl?gene=BEST1
C12orf65	https://www.genecards.org/cgi-bin/carddisp.pl?gene=C12orf65
C1QTNF5	https://www.genecards.org/cgi-bin/carddisp.pl?gene=C1QTNF5
C2	https://www.genecards.org/cgi-bin/carddisp.pl?gene=C2
C3	https://www.genecards.org/cgi-bin/carddisp.pl?gene=C3
C8orf37	https://www.genecards.org/cgi-bin/carddisp.pl?gene=C8orf37
CA4	https://www.genecards.org/cgi-bin/carddisp.pl?gene=CA4

CABP4	https://www.genecards.org/cgi-bin/carddisp.pl?gene=CABP4
CACNA1F	https://www.genecards.org/cgi-bin/carddisp.pl?gene=CACNA1F
CAPN5	https://www.genecards.org/cgi-bin/carddisp.pl?gene=CAPN5
CC2D2A	https://www.genecards.org/cgi-bin/carddisp.pl?gene=CC2D2A
CCT2	https://www.genecards.org/cgi-bin/carddisp.pl?gene=CCT2
CD36	https://www.genecards.org/cgi-bin/carddisp.pl?gene=CD36
CDH23	https://www.genecards.org/cgi-bin/carddisp.pl?gene=CDH23
CDH3	https://www.genecards.org/cgi-bin/carddisp.pl?gene=CDH3
CEP164	https://www.genecards.org/cgi-bin/carddisp.pl?gene=CEP164
CEP19	https://www.genecards.org/cgi-bin/carddisp.pl?gene=CEP19
CEP250	https://www.genecards.org/cgi-bin/carddisp.pl?gene=CEP250
CEP290	https://www.genecards.org/cgi-bin/carddisp.pl?gene=CEP290
CEP78	https://www.genecards.org/cgi-bin/carddisp.pl?gene=CEP78
CERKL	https://www.genecards.org/cgi-bin/carddisp.pl?gene=CERKL
CFB	https://www.genecards.org/cgi-bin/carddisp.pl?gene=CFB
CFD	https://www.genecards.org/cgi-bin/carddisp.pl?gene=CFD
CFH	https://www.genecards.org/cgi-bin/carddisp.pl?gene=CFH
CFHR1	https://www.genecards.org/cgi-bin/carddisp.pl?gene=CFHR1
CHM	https://www.genecards.org/cgi-bin/carddisp.pl?gene=CHM
CIB2	https://www.genecards.org/cgi-bin/carddisp.pl?gene=CIB2
CLCC1	https://www.genecards.org/cgi-bin/carddisp.pl?gene=CLCC1
CLN3	https://www.genecards.org/cgi-bin/carddisp.pl?gene=CLN3
CLRN1	https://www.genecards.org/cgi-bin/carddisp.pl?gene=CLRN1
CLUAP1	https://www.genecards.org/cgi-bin/carddisp.pl?gene=CLUAP1
CNGA1	https://www.genecards.org/cgi-bin/carddisp.pl?gene=CNGA1
CNGA3	https://www.genecards.org/cgi-bin/carddisp.pl?gene=CNGA3
CNGB1	https://www.genecards.org/cgi-bin/carddisp.pl?gene=CNGB1
CNGB3	https://www.genecards.org/cgi-bin/carddisp.pl?gene=CNGB3
CNNM4	https://www.genecards.org/cgi-bin/carddisp.pl?gene=CNNM4
COL11A1	https://www.genecards.org/cgi-bin/carddisp.pl?gene=COL11A1
COL2A1	https://www.genecards.org/cgi-bin/carddisp.pl?gene=COL2A1
COL9A1	https://www.genecards.org/cgi-bin/carddisp.pl?gene=COL9A1
COPB2	https://www.genecards.org/cgi-bin/carddisp.pl?gene=COPB2
COX1	https://www.genecards.org/cgi-bin/carddisp.pl?gene=COX1
COX2	https://www.genecards.org/cgi-bin/carddisp.pl?gene=COX2
CRB1	https://www.genecards.org/cgi-bin/carddisp.pl?gene=CRB1
CRX	https://www.genecards.org/cgi-bin/carddisp.pl?gene=CRX
CSPP1	https://www.genecards.org/cgi-bin/carddisp.pl?gene=CSPP1
CTNNA1	https://www.genecards.org/cgi-bin/carddisp.pl?gene=CTNNA1
CWC27	https://www.genecards.org/cgi-bin/carddisp.pl?gene=CWC27
CYP27A1	https://www.genecards.org/cgi-bin/carddisp.pl?gene=CYP27A1
CYP4V2	https://www.genecards.org/cgi-bin/carddisp.pl?gene=CYP4V2
DHDDS	https://www.genecards.org/cgi-bin/carddisp.pl?gene=DHDDS
DHRS13	https://www.genecards.org/cgi-bin/carddisp.pl?gene=DHRS13

DHRS3	https://www.genecards.org/cgi-bin/carddisp.pl?gene=DHRS3
DHRS4	https://www.genecards.org/cgi-bin/carddisp.pl?gene=DHRS4
DHRS9	https://www.genecards.org/cgi-bin/carddisp.pl?gene=DHRS9
DHX38	https://www.genecards.org/cgi-bin/carddisp.pl?gene=DHX38
DMD	https://www.genecards.org/cgi-bin/carddisp.pl?gene=DMD
DRAM2	https://www.genecards.org/cgi-bin/carddisp.pl?gene=DRAM2
DTHD1	https://www.genecards.org/cgi-bin/carddisp.pl?gene=DTHD1
DYNC2H1	https://www.genecards.org/cgi-bin/carddisp.pl?gene=DYNC2H1
DYNC2I2	https://www.genecards.org/cgi-bin/carddisp.pl?gene=DYNC2I2
EFEMP1	https://www.genecards.org/cgi-bin/carddisp.pl?gene=EFEMP1
ELOVL1	https://www.genecards.org/cgi-bin/carddisp.pl?gene=ELOVL1
ELOVL4	https://www.genecards.org/cgi-bin/carddisp.pl?gene=ELOVL4
EMC1	https://www.genecards.org/cgi-bin/carddisp.pl?gene=EMC1
ENSA	https://www.genecards.org/cgi-bin/carddisp.pl?gene=ENSA
ERCC6	https://www.genecards.org/cgi-bin/carddisp.pl?gene=ERCC6
ESPN	https://www.genecards.org/cgi-bin/carddisp.pl?gene=ESPN
EXOSC2	https://www.genecards.org/cgi-bin/carddisp.pl?gene=EXOSC2
EYS	https://www.genecards.org/cgi-bin/carddisp.pl?gene=EYS
FAM161A	https://www.genecards.org/cgi-bin/carddisp.pl?gene=FAM161A
FBLN5	https://www.genecards.org/cgi-bin/carddisp.pl?gene=FBLN5
FLVCR1	https://www.genecards.org/cgi-bin/carddisp.pl?gene=FLVCR1
FSCN2	https://www.genecards.org/cgi-bin/carddisp.pl?gene=FSCN2
FZD4	https://www.genecards.org/cgi-bin/carddisp.pl?gene=FZD4
GDF6	https://www.genecards.org/cgi-bin/carddisp.pl?gene=GDF6
GIP	https://www.genecards.org/cgi-bin/carddisp.pl?gene=GIP
GIPC1	https://www.genecards.org/cgi-bin/carddisp.pl?gene=GIPC1
GNAT1	https://www.genecards.org/cgi-bin/carddisp.pl?gene=GNAT1
GNAT2	https://www.genecards.org/cgi-bin/carddisp.pl?gene=GNAT2
GNB3	https://www.genecards.org/cgi-bin/carddisp.pl?gene=GNB3
GNPTG	https://www.genecards.org/cgi-bin/carddisp.pl?gene=GNPTG
GPR179	https://www.genecards.org/cgi-bin/carddisp.pl?gene=GPR179
GRK1	https://www.genecards.org/cgi-bin/carddisp.pl?gene=GRK1
GRM6	https://www.genecards.org/cgi-bin/carddisp.pl?gene=GRM6
GUCA1B	https://www.genecards.org/cgi-bin/carddisp.pl?gene=GUCA1B
GUCY2D	https://www.genecards.org/cgi-bin/carddisp.pl?gene=GUCY2D
HARS	https://www.genecards.org/cgi-bin/carddisp.pl?gene=HARS
HGSNAT	https://www.genecards.org/cgi-bin/carddisp.pl?gene=HGSNAT
HK1	https://www.genecards.org/cgi-bin/carddisp.pl?gene=HK1
HMCN1	https://www.genecards.org/cgi-bin/carddisp.pl?gene=HMCN1
HMX1	https://www.genecards.org/cgi-bin/carddisp.pl?gene=HMX1
HSD17B6	https://www.genecards.org/cgi-bin/carddisp.pl?gene=HSD17B6
HTRA1	https://www.genecards.org/cgi-bin/carddisp.pl?gene=HTRA1
IDH3B	https://www.genecards.org/cgi-bin/carddisp.pl?gene=IDH3B
IFT140	https://www.genecards.org/cgi-bin/carddisp.pl?gene=IFT140

IFT172	https://www.genecards.org/cgi-bin/carddisp.pl?gene=IFT172
IFT27	https://www.genecards.org/cgi-bin/carddisp.pl?gene=IFT27
IFT81	https://www.genecards.org/cgi-bin/carddisp.pl?gene=IFT81
IMPDH1	https://www.genecards.org/cgi-bin/carddisp.pl?gene=IMPDH1
IMPG1	https://www.genecards.org/cgi-bin/carddisp.pl?gene=IMPG1
INPP5E	https://www.genecards.org/cgi-bin/carddisp.pl?gene=INPP5E
INVS	https://www.genecards.org/cgi-bin/carddisp.pl?gene=INVS
IQCB1	https://www.genecards.org/cgi-bin/carddisp.pl?gene=IQCB1
ITM2B	https://www.genecards.org/cgi-bin/carddisp.pl?gene=ITM2B
JAG1	https://www.genecards.org/cgi-bin/carddisp.pl?gene=JAG1
KCNJ13	https://www.genecards.org/cgi-bin/carddisp.pl?gene=KCNJ13
KCNV2	https://www.genecards.org/cgi-bin/carddisp.pl?gene=KCNV2
KIAA1549	https://www.genecards.org/cgi-bin/carddisp.pl?gene=KIAA1549
KIF11	https://www.genecards.org/cgi-bin/carddisp.pl?gene=KIF11
KIF3B	https://www.genecards.org/cgi-bin/carddisp.pl?gene=KIF3B
KIZ	https://www.genecards.org/cgi-bin/carddisp.pl?gene=KIZ
KLHL7	https://www.genecards.org/cgi-bin/carddisp.pl?gene=KLHL7
KSS	https://www.genecards.org/cgi-bin/carddisp.pl?gene=KSS
LAMA1	https://www.genecards.org/cgi-bin/carddisp.pl?gene=LAMA1
LCA5	https://www.genecards.org/cgi-bin/carddisp.pl?gene=LCA5
LCN2	https://www.genecards.org/cgi-bin/carddisp.pl?gene=LCN2
LHON	https://www.genecards.org/cgi-bin/carddisp.pl?gene=LHON
LRAT	https://www.genecards.org/cgi-bin/carddisp.pl?gene=LRAT
LRIT3	https://www.genecards.org/cgi-bin/carddisp.pl?gene=LRIT3
LRP5	https://www.genecards.org/cgi-bin/carddisp.pl?gene=LRP5
LZTFL1	https://www.genecards.org/cgi-bin/carddisp.pl?gene=LZTFL1
MAK	https://www.genecards.org/cgi-bin/carddisp.pl?gene=MAK
MAPKAPK3	https://www.genecards.org/cgi-bin/carddisp.pl?gene=MAPKAPK3
MERTK	https://www.genecards.org/cgi-bin/carddisp.pl?gene=MERTK
MFN2	https://www.genecards.org/cgi-bin/carddisp.pl?gene=MFN2
MFRP	https://www.genecards.org/cgi-bin/carddisp.pl?gene=MFRP
MFSD8	https://www.genecards.org/cgi-bin/carddisp.pl?gene=MFSD8
MIEF1	https://www.genecards.org/cgi-bin/carddisp.pl?gene=MIEF1
MIR204	https://www.genecards.org/cgi-bin/carddisp.pl?gene=MIR204
MKKS	https://www.genecards.org/cgi-bin/carddisp.pl?gene=MKKS
MKS1	https://www.genecards.org/cgi-bin/carddisp.pl?gene=MKS1
MSTN	https://www.genecards.org/cgi-bin/carddisp.pl?gene=MSTN
MT-ATP6	https://www.genecards.org/cgi-bin/carddisp.pl?gene=MT-ATP6
MT-TH	https://www.genecards.org/cgi-bin/carddisp.pl?gene=MT-TH
MT-TL1	https://www.genecards.org/cgi-bin/carddisp.pl?gene=MT-TL1
MT-TP	https://www.genecards.org/cgi-bin/carddisp.pl?gene=MT-TP
MT-TS2	https://www.genecards.org/cgi-bin/carddisp.pl?gene=MT-TS2
MTTP	https://www.genecards.org/cgi-bin/carddisp.pl?gene=MTTP
MVK	https://www.genecards.org/cgi-bin/carddisp.pl?gene=MVK

MYO7A	https://www.genecards.org/cgi-bin/carddisp.pl?gene=MYO7A
NBAS	https://www.genecards.org/cgi-bin/carddisp.pl?gene=NBAS
NDP	https://www.genecards.org/cgi-bin/carddisp.pl?gene=NDP
NEK2	https://www.genecards.org/cgi-bin/carddisp.pl?gene=NEK2
NEUROD1	https://www.genecards.org/cgi-bin/carddisp.pl?gene=NEUROD1
NMNAT1	https://www.genecards.org/cgi-bin/carddisp.pl?gene=NMNAT1
NPHP1	https://www.genecards.org/cgi-bin/carddisp.pl?gene=NPHP1
NPHP3	https://www.genecards.org/cgi-bin/carddisp.pl?gene=NPHP3
NPHP4	https://www.genecards.org/cgi-bin/carddisp.pl?gene=NPHP4
NR2E3	https://www.genecards.org/cgi-bin/carddisp.pl?gene=NR2E3
NR2F1	https://www.genecards.org/cgi-bin/carddisp.pl?gene=NR2F1
NRL	https://www.genecards.org/cgi-bin/carddisp.pl?gene=NRL
NYX	https://www.genecards.org/cgi-bin/carddisp.pl?gene=NYX
OAT	https://www.genecards.org/cgi-bin/carddisp.pl?gene=OAT
OFD1	https://www.genecards.org/cgi-bin/carddisp.pl?gene=OFD1
OPA1	https://www.genecards.org/cgi-bin/carddisp.pl?gene=OPA1
OPA3	https://www.genecards.org/cgi-bin/carddisp.pl?gene=OPA3
OPN1LW	https://www.genecards.org/cgi-bin/carddisp.pl?gene=OPN1LW
OPN1MW	https://www.genecards.org/cgi-bin/carddisp.pl?gene=OPN1MW
OPN1SW	https://www.genecards.org/cgi-bin/carddisp.pl?gene=OPN1SW
OTX2	https://www.genecards.org/cgi-bin/carddisp.pl?gene=OTX2
PANK2	https://www.genecards.org/cgi-bin/carddisp.pl?gene=PANK2
PAX2	https://www.genecards.org/cgi-bin/carddisp.pl?gene=PAX2
PCARE	https://www.genecards.org/cgi-bin/carddisp.pl?gene=PCARE
PCDH15	https://www.genecards.org/cgi-bin/carddisp.pl?gene=PCDH15
PCYT1A	https://www.genecards.org/cgi-bin/carddisp.pl?gene=PCYT1A
PDE6A	https://www.genecards.org/cgi-bin/carddisp.pl?gene=PDE6A
PDE6B	https://www.genecards.org/cgi-bin/carddisp.pl?gene=PDE6B
PDE6C	https://www.genecards.org/cgi-bin/carddisp.pl?gene=PDE6C
PDE6G	https://www.genecards.org/cgi-bin/carddisp.pl?gene=PDE6G
PDE6H	https://www.genecards.org/cgi-bin/carddisp.pl?gene=PDE6H
PDZD7	https://www.genecards.org/cgi-bin/carddisp.pl?gene=PDZD7
PEX1	https://www.genecards.org/cgi-bin/carddisp.pl?gene=PEX1
PEX2	https://www.genecards.org/cgi-bin/carddisp.pl?gene=PEX2
PEX7	https://www.genecards.org/cgi-bin/carddisp.pl?gene=PEX7
PGK1	https://www.genecards.org/cgi-bin/carddisp.pl?gene=PGK1
PHYH	https://www.genecards.org/cgi-bin/carddisp.pl?gene=PHYH
PLA2G5	https://www.genecards.org/cgi-bin/carddisp.pl?gene=PLA2G5
PLK4	https://www.genecards.org/cgi-bin/carddisp.pl?gene=PLK4
PNPLA6	https://www.genecards.org/cgi-bin/carddisp.pl?gene=PNPLA6
POC1B	https://www.genecards.org/cgi-bin/carddisp.pl?gene=POC1B
POC5	https://www.genecards.org/cgi-bin/carddisp.pl?gene=POC5
POMGNT1	https://www.genecards.org/cgi-bin/carddisp.pl?gene=POMGNT1
PPT1	https://www.genecards.org/cgi-bin/carddisp.pl?gene=PPT1

PRCD	https://www.genecards.org/cgi-bin/carddisp.pl?gene=PRCD
PRDM13	https://www.genecards.org/cgi-bin/carddisp.pl?gene=PRDM13
PROM1	https://www.genecards.org/cgi-bin/carddisp.pl?gene=PROM1
PROS1	https://www.genecards.org/cgi-bin/carddisp.pl?gene=PROS1
PRPF3	https://www.genecards.org/cgi-bin/carddisp.pl?gene=PRPF3
PRPF31	https://www.genecards.org/cgi-bin/carddisp.pl?gene=PRPF31
PRPF4	https://www.genecards.org/cgi-bin/carddisp.pl?gene=PRPF4
PRPF6	https://www.genecards.org/cgi-bin/carddisp.pl?gene=PRPF6
PRPF8	https://www.genecards.org/cgi-bin/carddisp.pl?gene=PRPF8
PRPH2	https://www.genecards.org/cgi-bin/carddisp.pl?gene=PRPH2
PRPS1	https://www.genecards.org/cgi-bin/carddisp.pl?gene=PRPS1
PTPN9	https://www.genecards.org/cgi-bin/carddisp.pl?gene=PTPN9
RAB28	https://www.genecards.org/cgi-bin/carddisp.pl?gene=RAB28
RAX2	https://www.genecards.org/cgi-bin/carddisp.pl?gene=RAX2
RB1	https://www.genecards.org/cgi-bin/carddisp.pl?gene=RB1
RBP3	https://www.genecards.org/cgi-bin/carddisp.pl?gene=RBP3
RBP4	https://www.genecards.org/cgi-bin/carddisp.pl?gene=RBP4
RBP5	https://www.genecards.org/cgi-bin/carddisp.pl?gene=RBP5
RCBTB1	https://www.genecards.org/cgi-bin/carddisp.pl?gene=RCBTB1
RD3	https://www.genecards.org/cgi-bin/carddisp.pl?gene=RD3
RDH10	https://www.genecards.org/cgi-bin/carddisp.pl?gene=RDH10
RDH11	https://www.genecards.org/cgi-bin/carddisp.pl?gene=RDH11
RDH12	https://www.genecards.org/cgi-bin/carddisp.pl?gene=RDH12
RDH14	https://www.genecards.org/cgi-bin/carddisp.pl?gene=RDH14
RDH16	https://www.genecards.org/cgi-bin/carddisp.pl?gene=RDH16
RDH5	https://www.genecards.org/cgi-bin/carddisp.pl?gene=RDH5
REEP6	https://www.genecards.org/cgi-bin/carddisp.pl?gene=REEP6
RETSAT	https://www.genecards.org/cgi-bin/carddisp.pl?gene=RETSAT
RGR	https://www.genecards.org/cgi-bin/carddisp.pl?gene=RGR
RGS9	https://www.genecards.org/cgi-bin/carddisp.pl?gene=RGS9
RGS9BP	https://www.genecards.org/cgi-bin/carddisp.pl?gene=RGS9BP
RHO	https://www.genecards.org/cgi-bin/carddisp.pl?gene=RHO
RIMS2	https://www.genecards.org/cgi-bin/carddisp.pl?gene=RIMS2
RLBP1	https://www.genecards.org/cgi-bin/carddisp.pl?gene=RLBP1
RP1	https://www.genecards.org/cgi-bin/carddisp.pl?gene=RP1
RP1L1	https://www.genecards.org/cgi-bin/carddisp.pl?gene=RP1L1
RP2	https://www.genecards.org/cgi-bin/carddisp.pl?gene=RP2
RPE65	https://www.genecards.org/cgi-bin/carddisp.pl?gene=RPE65
RPGR	https://www.genecards.org/cgi-bin/carddisp.pl?gene=RPGR
RPGRIP1	https://www.genecards.org/cgi-bin/carddisp.pl?gene=RPGRIP1
RPGRIP1L	https://www.genecards.org/cgi-bin/carddisp.pl?gene=RPGRIP1L
RRH	https://www.genecards.org/cgi-bin/carddisp.pl?gene=RRH
RS1	https://www.genecards.org/cgi-bin/carddisp.pl?gene=RS1
RTN4IP1	https://www.genecards.org/cgi-bin/carddisp.pl?gene=RTN4IP1

SAG	https://www.genecards.org/cgi-bin/carddisp.pl?gene=SAG
SAMD11	https://www.genecards.org/cgi-bin/carddisp.pl?gene=SAMD11
SCT	https://www.genecards.org/cgi-bin/carddisp.pl?gene=SCT
SDCCAG8	https://www.genecards.org/cgi-bin/carddisp.pl?gene=SDCCAG8
SEMA4A	https://www.genecards.org/cgi-bin/carddisp.pl?gene=SEMA4A
SLC24A1	https://www.genecards.org/cgi-bin/carddisp.pl?gene=SLC24A1
SLC25A46	https://www.genecards.org/cgi-bin/carddisp.pl?gene=SLC25A46
SLC4A7	https://www.genecards.org/cgi-bin/carddisp.pl?gene=SLC4A7
SLC7A14	https://www.genecards.org/cgi-bin/carddisp.pl?gene=SLC7A14
SNRNP200	https://www.genecards.org/cgi-bin/carddisp.pl?gene=SNRNP200
SPATA7	https://www.genecards.org/cgi-bin/carddisp.pl?gene=SPATA7
SPP2	https://www.genecards.org/cgi-bin/carddisp.pl?gene=SPP2
TEAD1	https://www.genecards.org/cgi-bin/carddisp.pl?gene=TEAD1
TGIF	https://www.genecards.org/cgi-bin/carddisp.pl?gene=TGIF
TIMM8A	https://www.genecards.org/cgi-bin/carddisp.pl?gene=TIMM8A
TIMP3	https://www.genecards.org/cgi-bin/carddisp.pl?gene=TIMP3
TLR3	https://www.genecards.org/cgi-bin/carddisp.pl?gene=TLR3
TLR4	https://www.genecards.org/cgi-bin/carddisp.pl?gene=TLR4
TMEM126A	https://www.genecards.org/cgi-bin/carddisp.pl?gene=TMEM126A
TMEM216	https://www.genecards.org/cgi-bin/carddisp.pl?gene=TMEM216
TMEM237	https://www.genecards.org/cgi-bin/carddisp.pl?gene=TMEM237
TOPORS	https://www.genecards.org/cgi-bin/carddisp.pl?gene=TOPORS
TREX1	https://www.genecards.org/cgi-bin/carddisp.pl?gene=TREX1
TRIM32	https://www.genecards.org/cgi-bin/carddisp.pl?gene=TRIM32
TRNT1	https://www.genecards.org/cgi-bin/carddisp.pl?gene=TRNT1
TRPM1	https://www.genecards.org/cgi-bin/carddisp.pl?gene=TRPM1
TSPAN12	https://www.genecards.org/cgi-bin/carddisp.pl?gene=TSPAN12
TTC8	https://www.genecards.org/cgi-bin/carddisp.pl?gene=TTC8
TTLL5	https://www.genecards.org/cgi-bin/carddisp.pl?gene=TTLL5
TTPA	https://www.genecards.org/cgi-bin/carddisp.pl?gene=TTPA
TUB	https://www.genecards.org/cgi-bin/carddisp.pl?gene=TUB
TUBGCP4	https://www.genecards.org/cgi-bin/carddisp.pl?gene=TUBGCP4
TUBGCP6	https://www.genecards.org/cgi-bin/carddisp.pl?gene=TUBGCP6
TULP1	https://www.genecards.org/cgi-bin/carddisp.pl?gene=TULP1
USH1C	https://www.genecards.org/cgi-bin/carddisp.pl?gene=USH1C
USH1G	https://www.genecards.org/cgi-bin/carddisp.pl?gene=USH1G
USH2A	https://www.genecards.org/cgi-bin/carddisp.pl?gene=USH2A
VCAN	https://www.genecards.org/cgi-bin/carddisp.pl?gene=VCAN
VEGF	https://www.genecards.org/cgi-bin/carddisp.pl?gene=VEGF
WDPCP	https://www.genecards.org/cgi-bin/carddisp.pl?gene=WDPCP
WDR19	https://www.genecards.org/cgi-bin/carddisp.pl?gene=WDR19
WFS1	https://www.genecards.org/cgi-bin/carddisp.pl?gene=WFS1
WHRN	https://www.genecards.org/cgi-bin/carddisp.pl?gene=WHRN
ZNF408	https://www.genecards.org/cgi-bin/carddisp.pl?gene=ZNF408

ZNF423	https://www.genecards.org/cgi-bin/carddisp.pl?gene=ZNF423

TABLE 4. Demographic and Clinical Characteristics of the Analyzed Cohort.

Characteristic	Unhealthy patients (n=453)	Control patients(n=74)	*p*-value
Gender (Male/Female)	238/215 (53%/47%)	51/23 (69%/31%)	<0.05
Mean Age (years, Min–Max ± SD)	47 (11 – 102) ± 19	46 (8 – 86) ± 20	>0.05
Mean LE+RE (±SD)	4.44 ± 1.38	10 ± 0	<0.05
Mutated gene count	2.52 ± 1.67	4.96 ± 1.77	<0.05
"Pathogenicity weight" score	0.38 ± 0.13	0.18 ± 0.03	<0.05

TABLE 5. Correlation analysis results between retinal pathways and possible scientific rationale for the correlations.

Pathways	*r value*	Possible scientific rationale
Retinoid Cycle Disease Events and The Canonical Retinoid Cycle in Rods (Twilight Vision)	0.92	Abnormalities in the retinoid cycle are closely associated with the development and progression of retinal diseases.
Visual Phototransduction and Sensory Perception of Light Stimulus	0.99	Modulating phototransduction could influence sensory responses.
Visual Perception and Sensory Perception	0.99	Improvements in visual perception could positively impact broader sensory capabilities.
Photoreceptor Cell Maintenance and Retina Homeostasis	0.74	The maintenance of photoreceptor cells is essential for the overall health and homeostasis of the retina.

TABLE 6. Gene combinations in the twilight vision pathway present in unhealthy and not in control patients.

Combination	Gene 1	Variant 1	Gene 2	Variant 2	Patients
ABCA4, RBP3	ABCA4	NM_000350.3:c.5603 A>T	RBP3	NM_002900.3:c.3715C>T	1
ABCA4, RBP3	ABCA4	NM_000350.3:c.6148G>C	RBP3	NM_002900.3:c.3715C>T	2
ABCA4, RDH12	ABCA4	NM_000350.3:c.766G>T	RDH12	NM_152443.3:c.C184C>T, NM_152443.3:c.805_809del	3
ABCA4, RDH12	ABCA4	NM_000350.3:c.3936G>C, NM_000350.3:c.574G>A	RDH12	NM_152443.3:c.578G>A	4

TABLE 7. Synthetic Dataset. Summary of protein expression frequency, mean intensity, and standard deviation across the 500 synthetic samples. Due to its size, the complete version of the table is not included here but is available upon request.

TABLE 8. Selected proteins and their correlation with pathways associated with the pathogenesis of retinal dystrophies.

Pathway	Proteins
Inflammation	COX2, CFB, CFD, CFHR1, TIMP3, VEGFA, LTB4R, LTE4
Oxidative Stress	APOD, APOE, ARSG, HMCN1
Immunity	C2, C3
Apoptosis	CAPN5, TIMP3, RB1
Aging	APOE, ARMS2, PRPF4, GRK1
Visual Perception	CNGB3, GRK1, GUCY2D, PDE6B, PDE6C, RGS9BP, SAG, RGR, RP1L1, RPGR, NRL, AIPL1, CABP4, BEST1, CLRN1, RLBP1
Ciliopathy	ARL6, BBS10, BBS2, CC2D2A, CLUAP1, IFT27, NPHP1, POC1B, RPGR, TTC8, USH2A, ALMS1, ARL2BP, CLN3, PCARE, PDZD7, WDPCP, C8orf37

Lipid Metabolism	ABCC6, ACBD5, APOD, APOE, LRP5, PEX7
Cellular Transport	ACBD5, AFG3L2, CHM, CLCC1, CNNM4, CYSLT1R, ESPN, HGSNAT, LCA5, LRAT, LZTFL1, MYO7A, PDE6B, PDE6C, SDCCAG8, TUBGCP4, TUBGCP6, ITM2B, KLHL7, REEP6
Signal Transduction	NEK2, PRDM13, TSPAN12

TABLE 9. Machine learning models performance. Accuracy, precision, recall and F1 score are showed for the four tested machine learning models, Support Vector Machine (SVM), Random Forest (RF), Logistic Regression (LR), Extreme Gradient Boosting (XGBoost).

Model	**Accuracy (%)**	**Precision**	**Recall**	**F1 score**
SVM	69%	0.69	0.68	0.68
RF	64%	0.64	0.64	0.64
LR	72%	0.72	0.71	0.71
XGBoost	70%	0.70	0.69	0.69

FIGURES

FIGURE 1. This figure illustrates the steps for the mathematical model development, including “Pathogenicity weight” normalization, data transformation, data aggregation, and probabilistic modeling.

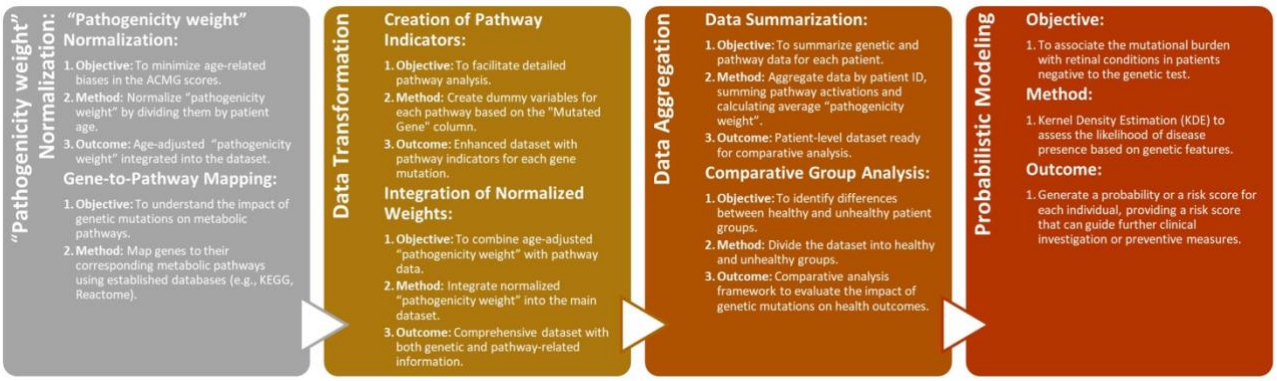

FIGURE 2. This figure shows the result of the Mann Whitney U test to compare the data from the interest group and the control group for each of the identified advantageous metabolic pathways. The two pathways that result significantly are: the canonical retinoid cycle in rods (twilight vision): p = 0.012084. Retinoid cycle disease events: p = 0.000002. The p-values are plotted on a logarithmic scale to highlight the most significant pathways.

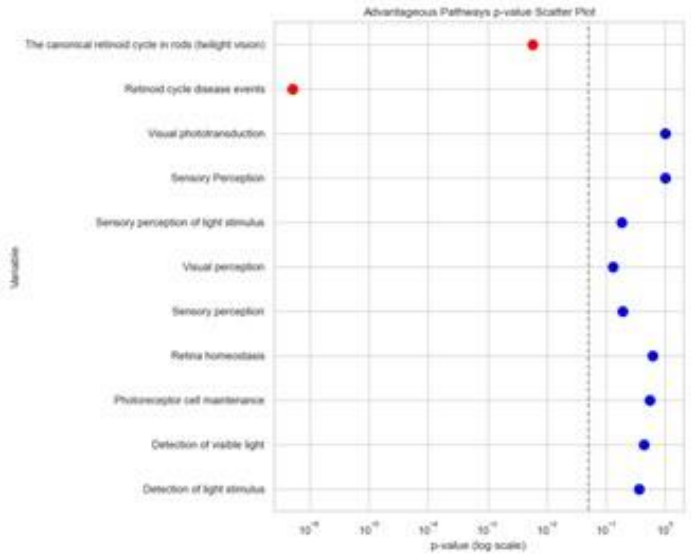

FIGURE 3. KDE curve delineates the density distribution of data points, and a vertical dashed line indicates the set threshold for patient classification. The X-axis represents the percentile rank estimated by the KDE for the average of the “pathogenicity weight” that summed for each variant in the target pathway, while the Y-axis indicates the estimated density. For higher accuracy in the significant pathway result, we use both Kernel density and U-Mann Whitney test. **A)** represents the KDE based on the canonical retinoid cycle in rods (twilight vision) pathway, and **B)** represents the Retinoid cycle disease events pathway.

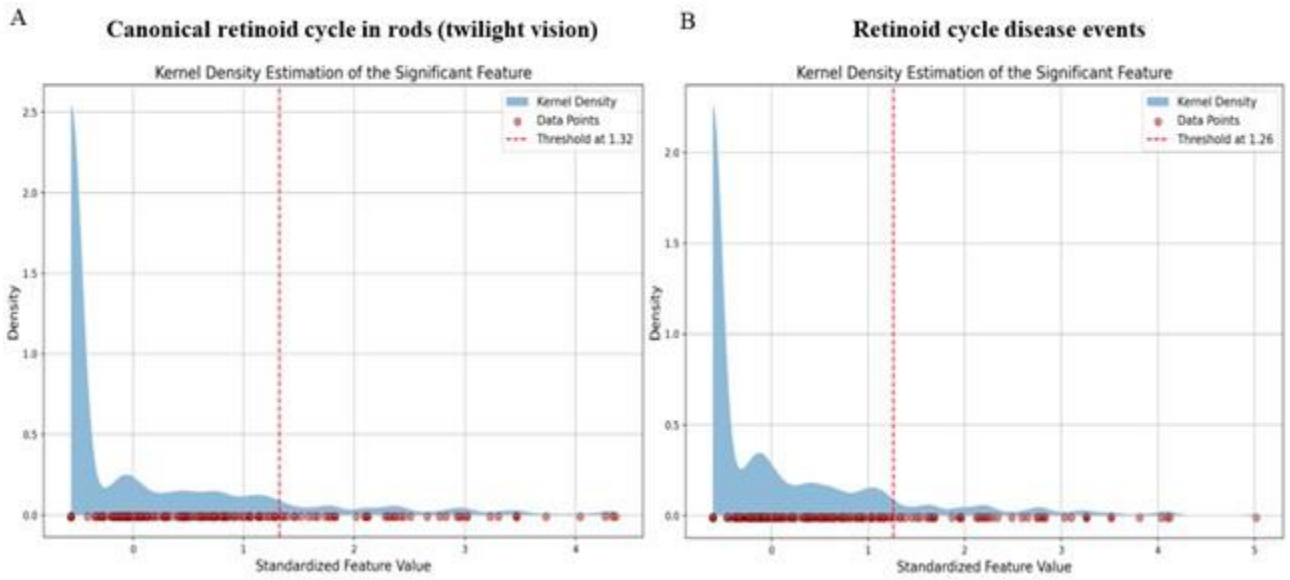

FIGURE 4. Flowchart of the model used to identify genetic combinations present in unhealthy patients but absent in controls. The process includes selecting patients with variants in genes from the twilight vision pathway, calculating genetic combinations in the analyzed cohorts, and selecting combinations exclusive to unhealthy patients.

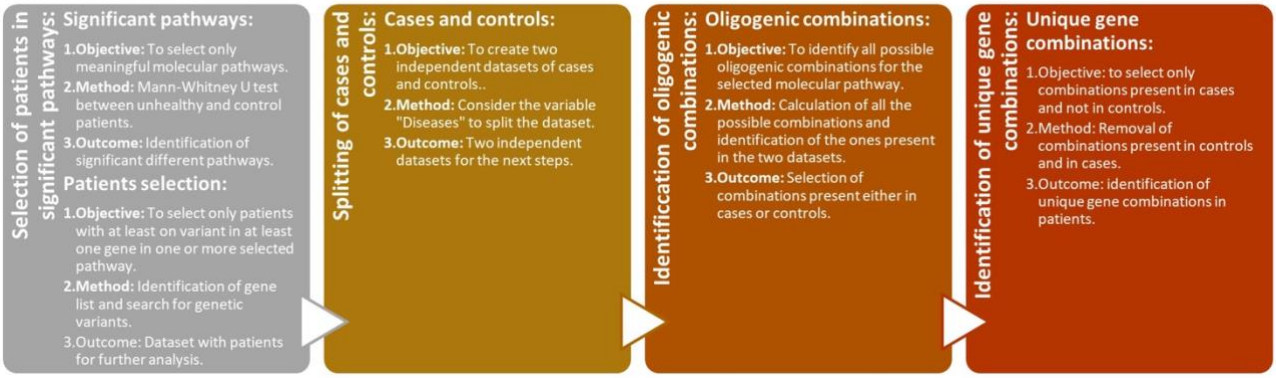

FIGURE 5. Proteins spectral counting distribution. Proteins are showed on the X axes, with their expression levels showed on the Y axes.

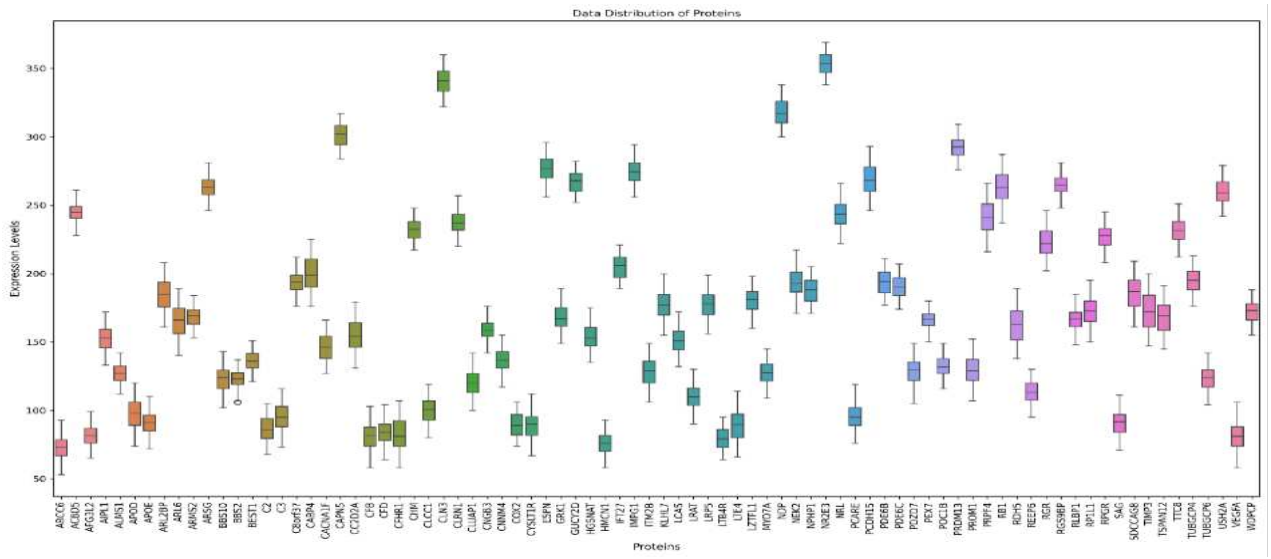

FIGURE 6. Confusion matrix of LR.

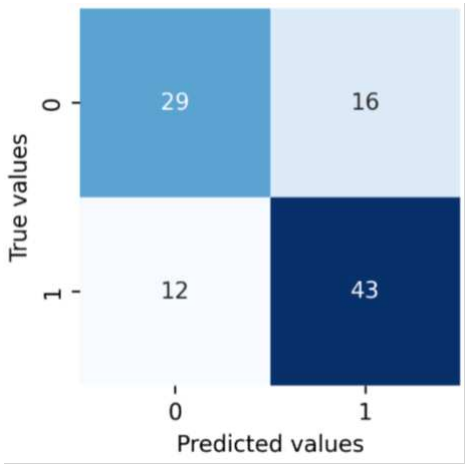

FIGURE 7. Feature Importance of LR, 15 most contributing proteins.

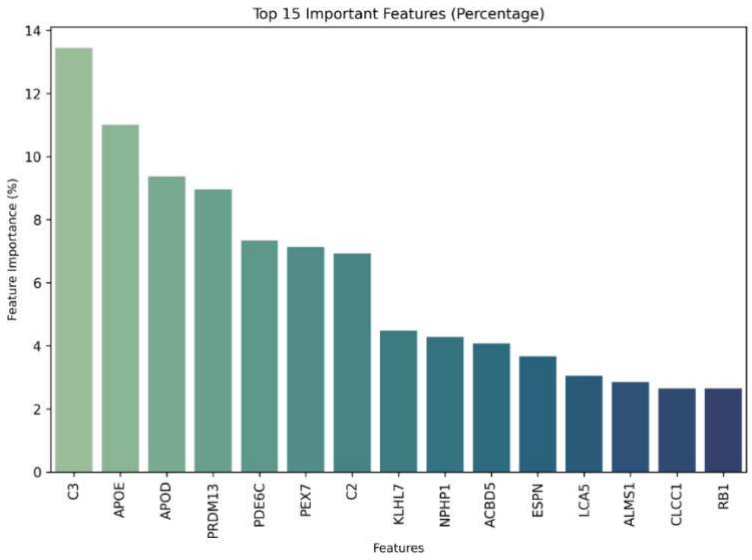

REFERENCES

[1] Manley, A., Meshkat, B. I., Jablonski, M. M., & Hollingsworth, T. J. (2023). Cellular and Molecular Mechanisms of Pathogenesis Underlying Inherited Retinal Dystrophies. *Biomolecules*, *13*(2), 271. https://doi.org/10.3390/biom13020271

[2] Colombo, L., Maltese, P. E., Castori, M., El Shamieh, S., Zeitz, C., Audo, I., Zulian, A., Marinelli, C., Benedetti, S., Costantini, A., Bressan, S., Percio, M., Ferri, P., Abeshi, A., Bertelli, M., & Rossetti, L. (2021). Molecular Epidemiology in 591 Italian Probands With Nonsyndromic Retinitis Pigmentosa and Usher Syndrome. Investigative ophthalmology & visual science, 62(2), 13. https://doi.org/10.1167/iovs.62.2.13

[3] Hejtmancik, J. F., & Daiger, S. P. (2020). Understanding the genetic architecture of human retinal degenerations. Proceedings of the National Academy of Sciences of the United States of America, 117(8), 3904–3906. https://doi.org/10.1073/pnas.1922925117

[4] Martin-Merida, I., Avila-Fernandez, A., Del Pozo-Valero, M., Blanco-Kelly, F., Zurita, O., Perez-Carro, R., Aguilera-Garcia, D., Riveiro-Alvarez, R., Arteche, A., Trujillo-Tiebas, M. J., Tahsin-Swafiri, S., Rodriguez-Pinilla, E., Lorda-Sanchez, I., Garcia-Sandoval, B., Corton, M., & Ayuso, C. (2019). Genomic Landscape of Sporadic Retinitis Pigmentosa: Findings from 877 Spanish Cases. Ophthalmology, 126(8), 1181–1188. https://doi.org/10.1016/j.ophtha.2019.03.018

[5] Rivolta, C., Celik, E., Kamdar, D., Cancellieri, F., Kaminska, K., Ullah, M., Barberán-Martínez, P., Bouckaert, M., Cortón, M., Delanote, E., Fernández-Caballero, L., García García, G., Holtes, L. K., Karali, M., Lopez, I., Peter, V. G., Schneider, N., Vincke, L., Ayuso, C., Banfi, S., … Quinodoz, M. (2025). RetiGene, a comprehensive gene atlas for inherited retinal diseases. American journal of human genetics, 112(10), 2253–2265. https://doi.org/10.1016/j.ajhg.2025.08.017

[6] Li, M. M., Datto, M., Duncavage, E. J., Kulkarni, S., Lindeman, N. I., Roy, S., Tsimberidou, A. M., Vnencak-Jones, C. L., Wolff, D. J., Younes, A., & Nikiforova, M. N. (2017). Standards and Guidelines for the Interpretation and Reporting of Sequence Variants in Cancer: A Joint Consensus Recommendation of the Association for Molecular Pathology, American Society of Clinical Oncology, and College of American Pathologists. The Journal of molecular diagnostics : JMD, 19(1), 4–23. https://doi.org/10.1016/j.jmoldx.2016.10.002

[7] González-Del Pozo, M., Fernández-Suárez, E., Martín-Sánchez, M., Bravo-Gil, N., Méndez-Vidal, C., Rodríguez-de la Rúa, E., Borrego, S., & Antiñolo, G. (2020). Unmasking Retinitis Pigmentosa complex cases by a whole genome sequencing algorithm based on open-access tools: hidden recessive inheritance and potential oligogenic variants. Journal of translational medicine, 18(1), 73. https://doi.org/10.1186/s12967-020-02258-3

[8] Boloc, D., Castillo-Lara, S., Marfany, G., Gonzàlez-Duarte, R., & Abril, J. F. (2015). Distilling a Visual Network of Retinitis Pigmentosa Gene-Protein Interactions to Uncover New Disease Candidates. PloS one, 10(8), e0135307. https://doi.org/10.1371/journal.pone.0135307

[9] Keith, B. P., Robertson, D. L., & Hentges, K. E. (2014). Locus heterogeneity disease genes encode proteins with high interconnectivity in the human protein interaction network. Frontiers in genetics, 5, 434. https://doi.org/10.3389/fgene.2014.00434

[10] Gamba, A., Salmona, M., & Bazzoni, G. (2020). Quantitative analysis of proteins which are members of the same protein complex but cause locus heterogeneity in disease. Scientific reports, 10(1), 10423. https://doi.org/10.1038/s41598-020-66836-7

[11] Eichers, E. R., Lewis, R. A., Katsanis, N., & Lupski, J. R. (2004). Triallelic inheritance: a bridge between Mendelian and multifactorial traits. Annals of medicine, 36(4), 262–272. https://doi.org/10.1080/07853890410026214

[12] Okazaki, A., & Ott, J. (2022). Machine learning approaches to explore digenic inheritance. Trends in genetics: TIG, 38(10), 1013–1018. https://doi.org/10.1016/j.tig.2022.04.009

[13] Messaoud, O., Dutta, A. K., Cornejo-Olivas, M. R., & Bhuiyan, Z. A. (2021). Editorial: Monogenic vs. Oligogenic Reclassification. Frontiers in genetics, 12, 821591. https://doi.org/10.3389/fgene.2021.821591

[14] Kajiwara, K., Berson, E. L., & Dryja, T. P. (1994). Digenic retinitis pigmentosa due to mutations at the unlinked peripherin/RDS and ROM1 loci. Science (New York, N.Y.), 264(5165), 1604–1608. https://doi.org/10.1126/science.8202715

[15] Liu, Y. P., Bosch, D. G., Siemiatkowska, A. M., Rendtorff, N. D., Boonstra, F. N., Möller, C., Tranebjærg, L., Katsanis, N., & Cremers, F. P. (2017). Putative digenic inheritance of

heterozygous RP1L1 and C2orf71 null mutations in syndromic retinal dystrophy. Ophthalmic genetics, 38(2), 127–132. https://doi.org/10.3109/13816810.2016.1151898

[16] Zheng, Q. Y., Yan, D., Ouyang, X. M., Du, L. L., Yu, H., Chang, B., Johnson, K. R., & Liu, X. Z. (2005). Digenic inheritance of deafness caused by mutations in genes encoding cadherin 23 and protocadherin 15 in mice and humans. Human molecular genetics, 14(1), 103–111. https://doi.org/10.1093/hmg/ddi010

[17] Ebermann, I., Phillips, J. B., Liebau, M. C., Koenekoop, R. K., Schermer, B., Lopez, I., Schäfer, E., Roux, A. F., Dafinger, C., Bernd, A., Zrenner, E., Claustres, M., Blanco, B., Nürnberg, G., Nürnberg, P., Ruland, R., Westerfield, M., Benzing, T., & Bolz, H. J. (2010). PDZD7 is a modifier of retinal disease and a contributor to digenic Usher syndrome. The Journal of clinical investigation, 120(6), 1812–1823. https://doi.org/10.1172/JCI39715

[18] Lee, J. E., Silhavy, J. L., Zaki, M. S., Schroth, J., Bielas, S. L., Marsh, S. E., Olvera, J., Brancati, F., Iannicelli, M., Ikegami, K., Schlossman, A. M., Merriman, B., Attié-Bitach, T., Logan, C. V., Glass, I. A., Cluckey, A., Louie, C. M., Lee, J. H., Raynes, H. R., Rapin, I., … Gleeson, J. G. (2012). CEP41 is mutated in Joubert syndrome and is required for tubulin glutamylation at the cilium. Nature genetics, 44(2), 193–199. https://doi.org/10.1038/ng.1078

[19] Guéant, J. L., Chéry, C., Oussalah, A., Nadaf, J., Coelho, D., Josse, T., Flayac, J., Robert, A., Koscinski, I., Gastin, I., Filhine-Tresarrieu, P., Pupavac, M., Brebner, A., Watkins, D., Pastinen, T., Montpetit, A., Hariri, F., Tregouët, D., Raby, B. A., Chung, W. K., … Rosenblatt, D. S. (2018). Publisher Correction: A PRDX1 mutant allele causes a MMACHC secondary epimutation in cblC patients. Nature communications, 9(1), 554. https://doi.org/10.1038/s41467-018-03054-w

[20] Beales, P. L., Badano, J. L., Ross, A. J., Ansley, S. J., Hoskins, B. E., Kirsten, B., Mein, C. A., Froguel, P., Scambler, P. J., Lewis, R. A., Lupski, J. R., & Katsanis, N. (2003). Genetic

interaction of BBS1 mutations with alleles at other BBS loci can result in non-Mendelian Bardet-Biedl syndrome. American journal of human genetics, 72(5), 1187–1199. https://doi.org/10.1086/375178

[21] Qin, M., Hayashi, H., Oshima, K., Tahira, T., Hayashi, K., & Kondo, H. (2005). Complexity of the genotype-phenotype correlation in familial exudative vitreoretinopathy with mutations in the LRP5 and/or FZD4 genes. Human mutation, 26(2), 104–112. https://doi.org/10.1002/humu.20191

[22] Yang, Y., Zhao, S., Zhang, Y., Wang, S., Shao, J., Liu, B., Li, Y., Yan, Z., Niu, Y., Li, X., Wang, L., Ye, Y., Weng, X., Wu, Z., Deciphering Disorders Involving Scoliosis and COmorbidities (DISCO) study, Zhang, J., & Wu, N. (2020). Mutational burden and potential oligogenic model of TBX6-mediated genes in congenital scoliosis. Molecular genetics & genomic medicine, 8(10), e1453. https://doi.org/10.1002/mgg3.1453

[23] Gazzo, A., Raimondi, D., Daneels, D., Moreau, Y., Smits, G., Van Dooren, S., & Lenaerts, T. (2017). Understanding mutational effects in digenic diseases. Nucleic acids research, 45(15), e140. https://doi.org/10.1093/nar/gkx557

[24] Yuan, Y., Zhang, L., Long, Q., Jiang, H., & Li, M. (2022). An accurate prediction model of digenic interaction for estimating pathogenic gene pairs of human diseases. Computational and structural biotechnology journal, 20, 3639–3652. https://doi.org/10.1016/j.csbj.2022.07.011

[25] Gonzaga-Jauregui, C., Harel, T., Gambin, T., Kousi, M., Griffin, L. B., Francescatto, L., Ozes, B., Karaca, E., Jhangiani, S. N., Bainbridge, M. N., Lawson, K. S., Pehlivan, D., Okamoto, Y., Withers, M., Mancias, P., Slavotinek, A., Reitnauer, P. J., Goksungur, M. T., Shy, M., Crawford, T. O., … Lupski, J. R. (2015). Exome Sequence Analysis Suggests that Genetic Burden Contributes to Phenotypic Variability and Complex Neuropathy. Cell reports, 12(7), 1169–1183. https://doi.org/10.1016/j.celrep.2015.07.023

[26] Kim, Y. J., Lee, J., Kim, N. Y., Hong, S., Cho, Y. S., & Yoon, J. (2021). The burden of rare damaging variants in hereditary atypical parkinsonism genes is increased in patients with Parkinson's disease. Neurobiology of aging, 100, 118.e5–118.e13. https://doi.org/10.1016/j.neurobiolaging.2020.11.011

[27] Amorim, C. E. G., Gao, Z., Baker, Z., Diesel, J. F., Simons, Y. B., Haque, I. S., Pickrell, J., & Przeworski, M. (2017). The population genetics of human disease: The case of recessive, lethal mutations. PLoS genetics, 13(9), e1006915. https://doi.org/10.1371/journal.pgen.1006915

[28] Bergendahl, L. T., Gerasimavicius, L., Miles, J., Macdonald, L., Wells, J. N., Welburn, J. P. I., & Marsh, J. A. (2019). The role of protein complexes in human genetic disease. Protein science : a publication of the Protein Society, 28(8), 1400–1411. https://doi.org/10.1002/pro.3667

[29] Hanany, M., Allon, G., Kimchi, A., Blumenfeld, A., Newman, H., Pras, E., Wormser, O., S Birk, O., Gradstein, L., Banin, E., Ben-Yosef, T., & Sharon, D. (2018). Carrier frequency analysis of mutations causing autosomal-recessive-inherited retinal diseases in the Israeli population. European journal of human genetics : EJHG, 26(8), 1159–1166. https://doi.org/10.1038/s41431-018-0152-0

[30] Hanany, M., Rivolta, C., & Sharon, D. (2020). Worldwide carrier frequency and genetic prevalence of autosomal recessive inherited retinal diseases. Proceedings of the National Academy of Sciences of the United States of America, 117(5), 2710–2716. https://doi.org/10.1073/pnas.1913179117

[31] Stunnenberg, H. G., & Hubner, N. C. (2014). Genomics meets proteomics: identifying the culprits in disease. Human genetics, 133(6), 689–700. https://doi.org/10.1007/s00439-013-1376-2

[32] Zenteno, J. C., García-Montaño, L. A., Cruz-Aguilar, M., Ronquillo, J., Rodas-Serrano, A., Aguilar-Castul, L., Matsui, R., Vencedor-Meraz, C. I., Arce-González, R., Graue-Wiechers, F., Gutiérrez-Paz, M., Urrea-Victoria, T., de Dios Cuadras, U., & Chacón-Camacho, O. F. (2020). Extensive genic and allelic heterogeneity underlying inherited retinal dystrophies in Mexican patients molecularly analyzed by next-generation sequencing. Molecular genetics & genomic medicine, 8(1), 10.1002/mgg3.1044. https://doi.org/10.1002/mgg3.1044

[33] Kolawole, O. U., Huang, A., Gregory-Evans, C. Y., Shunmugam, M., Weaver, T., & Gregory-Evans, K. (2024). Molecular genetic diagnostics for inherited retinal dystrophies in the clinical setting. Canadian journal of ophthalmology. Journal canadien d'ophtalmologie, 59(5), e575–e581. https://doi.org/10.1016/j.jcjo.2023.08.006

[34] Kaur, G., & Singh, N. K. (2023). Inflammation and retinal degenerative diseases. Neural regeneration research, 18(3), 513–518. https://doi.org/10.4103/1673-5374.350192

[35] Yu T-Y, Acosta ML, Ready S, et al. Light exposure causes functional changes in the retina: increased photoreceptor cation channel permeability, photoreceptor apoptosis, and altered retinal metabolic function. J Neurochem 2007;103:714–24.

[36] Colombo, L., Bonetti, G., Maltese, P. E., Iarossi, G., Ziccardi, L., Fogagnolo, P., De Ruvo, V., Murro, V., Giorgio, D., Falsini, B., Placidi, G., Martella, S., Galantin, E., Bertelli, M., & Rossetti, L. (2024). Genotypic and Phenotypic Characterization of a Cohort of Patients Affected by Rod Cyclic Nucleotide Channel-Associated Retinitis Pigmentosa. Ophthalmic research, 67(1), 301–310. https://doi.org/10.1159/000538746

[37] Bujakowska, K., Audo, I., Mohand-Saïd, S., Lancelot, M. E., Antonio, A., Germain, A., Léveillard, T., Letexier, M., Saraiva, J. P., Lonjou, C., Carpentier, W., Sahel, J. A., Bhattacharya, S. S., & Zeitz, C. (2012). CRB1 mutations in inherited retinal dystrophies. Human mutation, 33(2), 306–315. https://doi.org/10.1002/humu.21653

[38] Ehrenberg, M., Pierce, E. A., Cox, G. F., & Fulton, A. B. (2013). CRB1: one gene, many phenotypes. Seminars in ophthalmology, 28(5-6), 397–405. https://doi.org/10.3109/08820538.2013.825277

[39] Wu, L., Ueda, K., Nagasaki, T., & Sparrow, J. R. (2014). Light damage in Abca4 and Rpe65rd12 mice. Investigative ophthalmology & visual science, 55(3), 1910–1918. https://doi.org/10.1167/iovs.14-138674

[40] Yang, B., Yang, K., Chen, Y., Li, Q., Chen, J., Li, S., & Wu, Y. (2025). Exposure of A2E to blue light promotes ferroptosis in the retinal pigment epithelium. Cellular & molecular biology letters, 30(1), 22. https://doi.org/10.1186/s11658-025-00700-2

[41] Xu, H., & Chen, M. (2016). Targeting the complement system for the management of retinal inflammatory and degenerative diseases. European journal of pharmacology, 787, 94–104. https://doi.org/10.1016/j.ejphar.2016.03.001

[42] Hart, A. W., McKie, L., Morgan, J. E., Gautier, P., West, K., Jackson, I. J., & Cross, S. H. (2005). Genotype-phenotype correlation of mouse pde6b mutations. Investigative ophthalmology & visual science, 46(9), 3443–3450. https://doi.org/10.1167/iovs.05-0254

[43] Liu, H., Wang, M., Xia, C. H., Du, X., Flannery, J. G., Ridge, K. D., Beutler, B., & Gong, X. (2010). Severe retinal degeneration caused by a novel rhodopsin mutation. Investigative ophthalmology & visual science, 51(2), 1059–1065. https://doi.org/10.1167/iovs.09-3585

[44] Jacobson, S. G., Cideciyan, A. V., Huang, Y., Hanna, D. B., Freund, C. L., Affatigato, L. M., Carr, R. E., Zack, D. J., Stone, E. M., & McInnes, R. R. (1998). Retinal degenerations with truncation mutations in the cone-rod homeobox (CRX) gene. Investigative ophthalmology & visual science, 39(12), 2417–2426.

[45] Jones, B. W., Pfeiffer, R. L., Ferrell, W. D., Watt, C. B., Marmor, M., & Marc, R. E. (2016). Retinal remodeling in human retinitis pigmentosa. Experimental eye research, 150, 149–165. https://doi.org/10.1016/j.exer.2016.03.018

[46] Luthert, P. J., & Chong, N. H. (1998). Photoreceptor rescue. Eye (London, England), 12 (Pt 3b), 591–596. https://doi.org/10.1038/eye.1998.149

[47] Jones, B. W., Marc, R. E., & Pfeiffer, R. L. (2016). Retinal Degeneration, Remodeling and Plasticity. In H. Kolb (Eds.) et. al., Webvision: The Organization of the Retina and Visual System. University of Utah Health Sciences Center.

[48] Stone, J., Maslim, J., Valter-Kocsi, K., Mervin, K., Bowers, F., Chu, Y., Barnett, N., Provis, J., Lewis, G., Fisher, S. K., Bisti, S., Gargini, C., Cervetto, L., Merin, S., & Peér, J. (1999). Mechanisms of photoreceptor death and survival in mammalian retina. Progress in retinal and eye research, 18(6), 689–735. https://doi.org/10.1016/s1350-9462(98)00032-9

[49] Telias, M., Nawy, S., & Kramer, R. H. (2020). Degeneration-Dependent Retinal Remodeling: Looking for the Molecular Trigger. Frontiers in neuroscience, 14, 618019. https://doi.org/10.3389/fnins.2020.618019

[50] Marc, R. E., Jones, B. W., Watt, C. B., & Strettoi, E. (2003). Neural remodeling in retinal degeneration. Progress in retinal and eye research, 22(5), 607–655. https://doi.org/10.1016/s1350-9462(03)00039-9

[51] Country M. W. (2017). Retinal metabolism: A comparative look at energetics in the retina. Brain research, 1672, 50–57. https://doi.org/10.1016/j.brainres.2017.07.025

[52] Fu, Z., Kern, T. S., Hellström, A., & Smith, L. E. H. (2021). Fatty acid oxidation and photoreceptor metabolic needs. Journal of lipid research, 62, 100035. https://doi.org/10.1194/jlr.TR120000618

[53] Chen, X., Shi, C., He, M., Xiong, S., & Xia, X. (2023). Endoplasmic reticulum stress: molecular mechanism and therapeutic targets. Signal transduction and targeted therapy, 8(1), 352. https://doi.org/10.1038/s41392-023-01570-w

[54] Lin, J. H., & Lavail, M. M. (2010). Misfolded proteins and retinal dystrophies. Advances in experimental medicine and biology, 664, 115–121. https://doi.org/10.1007/978-1-4419-1399-9_14

[55] Ferrington, D. A., Fisher, C. R., & Kowluru, R. A. (2020). Mitochondrial Defects Drive Degenerative Retinal Diseases. Trends in molecular medicine, 26(1), 105–118. https://doi.org/10.1016/j.molmed.2019.10.008

[56] Parameswarappa, D. C., Kulkarni, A., Sahoo, N. K., Padhy, S. K., Singh, S. R., Héon, E., & Chhablani, J. (2024). From Cellular to Metabolic: Advances in Imaging of Inherited Retinal Diseases. Diagnostics (Basel, Switzerland), 15(1), 28. https://doi.org/10.3390/diagnostics15010028

[57] Guziewicz, K. E., Sinha, D., Gómez, N. M., Zorych, K., Dutrow, E. V., Dhingra, A., Mullins, R. F., Stone, E. M., Gamm, D. M., Boesze-Battaglia, K., & Aguirre, G. D. (2017). Bestrophinopathy: An RPE-photoreceptor interface disease. Progress in retinal and eye research, 58, 70–88. https://doi.org/10.1016/j.preteyeres.2017.01.005

[58] Holz, F. G., Pauleikhoff, D., Klein, R., & Bird, A. C. (2004). Pathogenesis of lesions in late age-related macular disease. American journal of ophthalmology, 137(3), 504–510. https://doi.org/10.1016/j.ajo.2003.11.026

[59] Hyttinen, J. M. T., Blasiak, J., & Kaarniranta, K. (2023). Non-Coding RNAs Regulating Mitochondrial Functions and the Oxidative Stress Response as Putative Targets against Age-Related Macular Degeneration (AMD). International journal of molecular sciences, 24(3), 2636. https://doi.org/10.3390/ijms24032636

[60] Garces, F. A., Scortecci, J. F., & Molday, R. S. (2020). Functional Characterization of ABCA4 Missense Variants Linked to Stargardt Macular Degeneration. International journal of molecular sciences, 22(1), 185. https://doi.org/10.3390/ijms22010185

[61] Farnoodian, M., Bose, D., Barone, F., Nelson, L. M., Boyle, M., Jun, B., Do, K., Gordon, W., Guerin, M. K., Perera, R., Ji, J. X., Cogliati, T., Sharma, R., Brooks, B. P., Bazan, N. G., & Bharti, K. (2023). Retina and RPE lipid profile changes linked with ABCA4 associated Stargardt's maculopathy. Pharmacology & therapeutics, 249, 108482. https://doi.org/10.1016/j.pharmthera.2023.108482

[62] Radu, R. A., Hu, J., Yuan, Q., Welch, D. L., Makshanoff, J., Lloyd, M., McMullen, S., Travis, G. H., & Bok, D. (2011). Complement system dysregulation and inflammation in the retinal pigment epithelium of a mouse model for Stargardt macular degeneration. The Journal of biological chemistry, 286(21), 18593–18601. https://doi.org/10.1074/jbc.M110.191866

[63] Kassa, E., Ciulla, T. A., Hussain, R. M., & Dugel, P. U. (2019). Complement inhibition as a therapeutic strategy in retinal disorders. Expert opinion on biological therapy, 19(4), 335–342. https://doi.org/10.1080/14712598.2019.1575358

[64] B Domènech, E., & Marfany, G. (2020). The Relevance of Oxidative Stress in the Pathogenesis and Therapy of Retinal Dystrophies. Antioxidants (Basel, Switzerland), 9(4), 347. https://doi.org/10.3390/antiox9040347

[65] Yang, X., Yu, X. W., Zhang, D. D., & Fan, Z. G. (2020). Blood-retinal barrier as a converging pivot in understanding the initiation and development of retinal diseases. Chinese medical journal, 133(21), 2586–2594. https://doi.org/10.1097/CM9.0000000000001015

[66] Rashid, K., Akhtar-Schaefer, I., & Langmann, T. (2019). Microglia in Retinal Degeneration. Frontiers in immunology, 10, 1975. https://doi.org/10.3389/fimmu.2019.01975

[67] Xu, X. R., Zhong, L., Huang, B. L., Wei, Y. H., Zhou, X., Wang, L., & Wang, F. Q. (2014). Comparative proteomic analysis of plasma proteins in patients with age-related macular

degeneration. International journal of ophthalmology, 7(2), 256–263. https://doi.org/10.3980/j.issn.2222-3959.2014.02.12

[68] Velez, G., Machlab, D. A., Tang, P. H., Sun, Y., Tsang, S. H., Bassuk, A. G., & Mahajan, V. B. (2018). Proteomic analysis of the human retina reveals region-specific susceptibilities to metabolic- and oxidative stress-related diseases. PloS one, 13(2), e0193250. https://doi.org/10.1371/journal.pone.0193250

[69] Youngblood, H., Robinson, R., Sharma, A., & Sharma, S. (2019). Proteomic Biomarkers of Retinal Inflammation in Diabetic Retinopathy. International journal of molecular sciences, 20(19), 4755. https://doi.org/10.3390/ijms20194755

[70] Lynch, A. M., Wagner, B. D., Palestine, A. G., Janjic, N., Patnaik, J. L., Mathias, M. T., Siringo, F. S., & Mandava, N. (2020). Plasma Biomarkers of Reticular Pseudodrusen and the Risk of Progression to Advanced Age-Related Macular Degeneration. Translational vision science & technology, 9(10), 12. https://doi.org/10.1167/tvst.9.10.12

[71] Moekotte, L., de Boer, J. H., Hiddingh, S., de Ligt, A., Nguyen, X. T., Hoyng, C. B., Inglehearn, C. F., McKibbin, M., Lamey, T. M., Thompson, J. A., Chen, F. K., McLaren, T. L., AlTalbishi, A., Panneman, D. M., Boonen, E. G. M., Banfi, S., Bocquet, B., Meunier, I., De Baere, E., Koenekoop, R., … Kuiper, J. J. W. (2025). Elevated Plasma Complement Factors in CRB1-Associated Inherited Retinal Dystrophies. Investigative ophthalmology & visual science, 66(2), 55. https://doi.org/10.1167/iovs.66.2.55

[72] Garzone, D., Finger, R. P., Mauschitz, M. M., Santos, M. L. S., Breteler, M. M. B., & Aziz, N. A. (2022). Neurofilament light chain and retinal layers' determinants and association: A population-based study. Annals of clinical and translational neurology, 9(4), 564–569. https://doi.org/10.1002/acn3.51522

[73] Flores, R., Carneiro, Â., Tenreiro, S., & Seabra, M. C. (2021). Retinal Progression Biomarkers of Early and Intermediate Age-Related Macular Degeneration. Life (Basel, Switzerland), 12(1), 36. https://doi.org/10.3390/life12010036

[74] García-Quintanilla, L., Rodríguez-Martínez, L., Bandín-Vilar, E., Gil-Martínez, M., González-Barcia, M., Mondelo-García, C., Fernández-Ferreiro, A., & Mateos, J. (2022). Recent Advances in Proteomics-Based Approaches to Studying Age-Related Macular Degeneration: A Systematic Review. International journal of molecular sciences, 23(23), 14759. https://doi.org/10.3390/ijms232314759

[75] Roberts, P. A., Gaffney, E. A., Whiteley, J. P., Luthert, P. J., Foss, A. J. E., & Byrne, H. M. (2018). Predictive Mathematical Models for the Spread and Treatment of Hyperoxia-induced Photoreceptor Degeneration in Retinitis Pigmentosa. Investigative ophthalmology & visual science, 59(3), 1238–1249. https://doi.org/10.1167/iovs.17-23177

[76] Camacho ET, Dobreva A, Larripa K, et al. Mathematical Modeling of Retinal Degeneration: Aerobic Glycolysis in a Single Cone, 2021, p. 135–78.

[77] Collin, G. B., Gogna, N., Chang, B., Damkham, N., Pinkney, J., Hyde, L. F., Stone, L., Naggert, J. K., Nishina, P. M., & Krebs, M. P. (2020). Mouse Models of Inherited Retinal Degeneration with Photoreceptor Cell Loss. Cells, 9(4), 931. https://doi.org/10.3390/cells9040931

[78] Cristofoli, F., Daja, M., Maltese, P. E., Guerri, G., Tanzi, B., Miotto, R., Bonetti, G., Miertus, J., Chiurazzi, P., Stuppia, L., Gatta, V., Cecchin, S., Bertelli, M., & Marceddu, G. (2023). MAGI-ACMG: Algorithm for the Classification of Variants According to ACMG and ACGS Recommendations. Genes, 14(8), 1600. https://doi.org/10.3390/genes14081600

[79] Collin, G. B., Gogna, N., Chang, B., Damkham, N., Pinkney, J., Hyde, L. F., Stone, L., Naggert, J. K., Nishina, P. M., & Krebs, M. P. (2020). Mouse Models of Inherited Retinal

Degeneration with Photoreceptor Cell Loss. Cells, 9(4), 931. https://doi.org/10.3390/cells9040931

[80] Huang, Z., & Wang, C. (2022). A Review on Differential Abundance Analysis Methods for Mass Spectrometry-Based Metabolomic Data. Metabolites, 12(4), 305. https://doi.org/10.3390/metabo12040305

[81] Iragavarapu, S., & Gorin, M. B. (2015). Gender specific issues in hereditary ocular disorders. Current eye research, 40(2), 128–145. https://doi.org/10.3109/02713683.2014.932813

[82] Haim, M., Holm, N. V., & Rosenberg, T. (1992). Prevalence of retinitis pigmentosa and allied disorders in Denmark. I Main results. Acta ophthalmologica, 70(2), 178–186. https://doi.org/10.1111/j.1755-3768.1992.tb04121.x

[83] Furlong L. I. (2013). Human diseases through the lens of network biology. Trends in genetics : TIG, 29(3), 150–159. https://doi.org/10.1016/j.tig.2012.11.004

[84] Pounraja, V. K., & Girirajan, S. (2022). A general framework for identifying oligogenic combinations of rare variants in complex disorders. Genome research, 32(5), 904–915. https://doi.org/10.1101/gr.276348.121

[85] Poloschek, C. M., Bach, M., Lagrèze, W. A., Glaus, E., Lemke, J. R., Berger, W., & Neidhardt, J. (2010). ABCA4 and ROM1: implications for modification of the PRPH2-associated macular dystrophy phenotype. Investigative ophthalmology & visual science, 51(8), 4253–4265. https://doi.org/10.1167/iovs.09-4655

[86] Lee, W., Paavo, M., Zernant, J., Stong, N., Laurente, Z., Bearelly, S., Nagasaki, T., Tsang, S. H., Goldstein, D. B., & Allikmets, R. (2019). Modification of the PROM1 disease phenotype by a mutation in ABCA4. Ophthalmic genetics, 40(4), 369–375. https://doi.org/10.1080/13816810.2019.1660382

[87] Zernant, J., Lee, W., Wang, J., Goetz, K., Ullah, E., Nagasaki, T., Su, P. Y., Fishman, G. A., Tsang, S. H., Tumminia, S. J., Brooks, B. P., Hufnagel, R. B., Chen, R., & Allikmets, R. (2022). Rare and common variants in ROM1 and PRPH2 genes trans-modify Stargardt/ABCA4 disease. PLoS genetics, 18(3), e1010129. https://doi.org/10.1371/journal.pgen.1010129

[88] Liu, Y., Chen, Y., Zhang, J., Liu, Y., Zhang, Y., & Su, Z. (2017). Retinoic acid receptor-related orphan receptor α stimulates adipose tissue inflammation by modulating endoplasmic reticulum stress. The Journal of biological chemistry, 292(34), 13959–13969. https://doi.org/10.1074/jbc.M117.782391

[89] Maeda, A., Golczak, M., Maeda, T., & Palczewski, K. (2009). Limited roles of Rdh8, Rdh12, and Abca4 in all-trans-retinal clearance in mouse retina. Investigative ophthalmology & visual science, 50(11), 5435–5443. https://doi.org/10.1167/iovs.09-3944

[90] Li, Z., Zhao, S., Cai, S., Zhang, Y., Wang, L., Niu, Y., Li, X., Hu, J., Chen, J., Wang, S., Wang, H., Liu, G., Tian, Y., Wu, Z., Zhang, T. J., DISCO (Deciphering Disorders Involving Scoliosis and COmorbidities) study, Wang, Y., & Wu, N. (2020). The mutational burden and oligogenic inheritance in Klippel-Feil syndrome. BMC musculoskeletal disorders, 21(1), 220. https://doi.org/10.1186/s12891-020-03229-x

[91] Cheng, Y., Cheng, T., & Qu, Y. (2019). TIMP-3 suppression induces choroidal neovascularization by moderating the polarization of macrophages in age-related macular degeneration. Molecular immunology, 106, 119–126. https://doi.org/10.1016/j.molimm.2018.12.026

[92] Aiello, L. P., Avery, R. L., Arrigg, P. G., Keyt, B. A., Jampel, H. D., Shah, S. T., Pasquale, L. R., Thieme, H., Iwamoto, M. A., & Park, J. E. (1994). Vascular endothelial growth factor in ocular fluid of patients with diabetic retinopathy and other retinal disorders. The New

England journal of medicine, 331(22), 1480–1487. https://doi.org/10.1056/NEJM199412013312203

[93] Tuxworth, R. I., Chen, H., Vivancos, V., Carvajal, N., Huang, X., & Tear, G. (2011). The Batten disease gene CLN3 is required for the response to oxidative stress. Human molecular genetics, 20(10), 2037–2047. https://doi.org/10.1093/hmg/ddr088

[94] Mahajan, V. B., Skeie, J. M., Bassuk, A. G., Fingert, J. H., Braun, T. A., Daggett, H. T., Folk, J. C., Sheffield, V. C., & Stone, E. M. (2012). Calpain-5 mutations cause autoimmune uveitis, retinal neovascularization, and photoreceptor degeneration. PLoS genetics, 8(10), e1003001. https://doi.org/10.1371/journal.pgen.1003001

[95] Casamassimi, A., Rienzo, M., Di Zazzo, E., Sorrentino, A., Fiore, D., Proto, M. C., Moncharmont, B., Gazzerro, P., Bifulco, M., & Abbondanza, C. (2020). Multifaceted Role of PRDM Proteins in Human Cancer. International journal of molecular sciences, 21(7), 2648. https://doi.org/10.3390/ijms21072648